Scalable, rapid and highly sensitive isothermal detection of SARS-CoV-2 for laboratory and home testing

Max J. Kellner[1,2,3#]*, James J. Ross[2#], Jakob Schnabl[2#], Marcus P.S. Dekens[1], Robert Heinen[1,2], Nathan A. Tanner[4], Robert Fritsche-Polanz[5], Marianna Traugott[6], Tamara Seitz[6], Alexander Zoufaly[6], Manuela Födinger[5,7], Christoph Wenisch[6], Johannes Zuber[1,8], Vienna Covid-19 Diagnostics Initiative (VCDI), Andrea Pauli[1]* & Julius Brennecke[2]*

[1]   Research Institute of Molecular Pathology (IMP), Vienna BioCenter (VBC), Campus-Vienna-Biocenter 1, 1030 Vienna, Austria.
[2]   Institute of Molecular Biotechnology of the Austrian Academy of Sciences (IMBA), Vienna BioCenter (VBC), Dr. Bohr-Gasse 3, 1030 Vienna, Austria.
[3]   MRC Laboratory of Molecular Biology, Francis Crick Avenue, Cambridge CB2 0QH, UK.
[4]   New England Biolabs (NEB), 240 County Road, Ipswich, MA, 01938, USA.
[5]   Institute of Laboratory Diagnostics, Klinik Favoriten, 1100 Vienna, Austria.
[6]   4th Medical Department with Infectious Diseases and Tropical Medicine, Klinik Favoriten, 1100 Vienna, Austria.
[7]   Sigmund Freud Private University, 1020 Vienna, Austria.
[8]   Medical University of Vienna, Vienna BioCenter (VBC), 1030 Vienna, Austria.

# equal contribution
* corresponding authors

Correspondence should be addressed to:
mkellner@mrc-lmb.cam.ac.uk, andrea.pauli@imp.ac.at, julius.brennecke@imba.oeaw.ac.at

Abstract

Global efforts to monitor and contain the Covid-19 pandemic, caused by the beta-coronavirus SARS-CoV-2, currently rely on RT-qPCR-based diagnostic assays. Yet their high cost, moderate throughput, and dependence on sophisticated equipment limit a broad implementation. Loop-mediated isothermal amplification (RT-LAMP) is an alternative detection method that has the potential to overcome these limitations. Here, we established a robust, highly sensitive and versatile RT-LAMP-based SARS-CoV-2 detection assay that is insensitive to carry-over contaminations. Our approach uses a rapid upfront lysis step and hydroxy-naphthol-blue (HNB) for colorimetric detection, which enables the robust identification of Covid-19 infections from a variety of sample types within 30 minutes. By combining RT-LAMP with a simple nucleic acid enrichment method (bead-LAMP), we profoundly increased assay sensitivity to RT-qPCR-like levels, thereby extending applications to large-scale pooled testing. Finally, we developed HomeDip-LAMP for pipette-free SARS-CoV-2 detection for low-resource environments. Our combined optimizations set the stage for implementing RT-LAMP as SARS-CoV-2 diagnostics assay for population-wide and home-based testing.

Keywords: Covid-19 diagnostics, Coronavirus, SARS-CoV-2, RT-LAMP, isothermal amplification

Introduction

The Covid-19 pandemic, caused by infection with the single-stranded, positive-sense RNA beta-coronavirus SARS-CoV-2, poses great global health and economic challenges (Gorbalenya et al., 2020). In the absence of effective treatment or vaccines, efforts to contain the spread of SARS-CoV-2 rely on systematic viral testing, contact tracing and isolation of infected individuals (Ferretti et al., 2020). Since SARS-CoV-2 carriers can be asymptomatic despite being infectious, a key challenge is to develop affordable and scalable technologies that enable population-wide testing (L. Zou et al., 2020). The gold-standard technique to detect an acute SARS-CoV-2 infection relies on nucleic acid diagnostics by RT-qPCR, which has been the method of choice due to its large dynamic range and high specificity (Corman et al., 2020). However, the need for specialized equipment and associated high cost make this technology unsuitable for population-scale testing, low resource settings and home testing. Moreover, slow turn-around times of several hours limit the applicability of RT-qPCR-based testing for situations where rapid screening is needed (CDC, 2020).

Isothermal nucleic acid amplification techniques, such as RPA (Recombinase-based Polymerase Amplification) (Piepenburg, Williams, Stemple, & Armes, 2006) or LAMP (Loop mediated isothermal amplification)

(Notomi et al., 2000), have great potential to fill the technological gap required for large scale testing strategies as they enable rapid nucleic acid diagnostics with minimal equipment requirement (Niemz, Ferguson, & Boyle, 2011). Coupled to a reverse transcriptase step that converts viral RNA into single stranded DNA, several LAMP protocols for SARS-CoV-2 detection have been developed and applied to patient testing (Anahtar et al., 2020; Butler et al., 2020; Rabe & Cepko, 2020). Innovations such as a colorimetric read-out or the combination of RT-LAMP with specific CRISPR-Cas enzymatic detection has further simplified the assay and enhanced specificity, respectively (Broughton et al., 2020; Zhang, Odiwuor, et al., 2020; Zhang, Ren, et al., 2020). However, several challenges remain, especially in terms of robustness of the assay, compatibility with crude patient samples, limitations in sensitivity, and making RT-LAMP compatible with home testing setups. Considering robustness, a rarely discussed problem is that performing RT-LAMP outside certified diagnostic laboratories can easily lead to carryover cross-contamination, resulting in potentially large numbers of false positives (Hsieh, Mage, Csordas, Eisenstein, & Tom Soh, 2014). Especially for pooled testing strategies where each patient from a positive pool must subsequently be tested individually for the presence of viral RNA, this poses a great challenge. Moreover, the currently used colorimetric RT-LAMP assay for SARS-CoV-2 detection relies on a pH-indicator that, depending on the input sample, often requires careful adjustment of sample pH and buffer capacity (Rabe & Cepko, 2020). Considering sensitivity, current RT-LAMP assays are one to two orders of magnitudes less sensitive compared to RT-qPCR, leading to considerable numbers of false negatives (Anahtar et al., 2020; Broughton et al., 2020). Limited sensitivity has been a major obstacle to making RT-LAMP-based testing competitive for SARS-CoV-2 diagnostics and screening efforts. When home testing is considered, setting up isothermal RT-LAMP reactions still requires basic laboratory equipment such as pipettes to transfer µl-scale sample volumes.

Here, we present a series of improvements that overcome the afore mentioned limitations of current RT-LAMP-based SARS-CoV-2 detection. We adopt an approach to greatly reduce the risk of carry-over contamination for SARS-CoV-2 testing, increase the robustness of the assay across all tested sample types and buffer conditions by using hydroxynaphtholblue (HNB) as colorimetric readout, greatly boost sensitivity by combining RT-LAMP with a simple RNA enrichment procedure, and finally benchmark a pipette-free method that enables sensitive and specific detection of SARS-CoV-2 in home settings.

Results

SARS-CoV-2 diagnostics relies on detection of viral RNA through reverse transcription and subsequent amplification of small parts of the 30 kilobase viral genome. Transcriptomic studies of SARS-CoV-2 infected human cells demonstrated the differential abundance of subgenomic viral RNAs, with transcripts at the 3' end of the viral genome being more abundant

(Kim et al., 2020). We first benchmarked published SARS-CoV-2 specific primer sets targeting different regions of the viral genome, the 5'-located ORF1ab, the envelope E-gene and the most 3'-located N-gene encoding the nucleocapsid protein (**Figure 1A**) (Broughton et al., 2020; Rabe & Cepko, 2020; Zhang, Odiwuor, et al., 2020; Zhang, Ren, et al., 2020). We used RNA extracted from nasopharyngeal swabs obtained from Covid-19 infected patients or confirmed Covid-19 negative individuals (negative controls) and a SARS-CoV-2 genomic RNA standard to determine primer specificity and sensitivity in RT-LAMP reactions with fluorometric real-time readout. None of the primer pairs resulted in non-specific amplification within the first 50 minutes in negative controls, indicative of their high specificity. In contrast, when patient RNA or synthetic SARS-CoV-2 standard was used as input, robust target amplification occurred within the first 10-20 minutes (**Figure 1B, S1A, B**). Recording measurements in real-time or as end-point analysis within 30-35 minutes reaction time is therefore robust and was used throughout this study. All primers tested yielded specific amplification of synthetic RNA standard with a sensitivity of at least ~1.000 copies per reaction, corresponding to a RT-qPCR measured Cq of ~30 (**Figure S1B, S5B**). Three primer sets enabled SARS-CoV-2 detection down to ~16 copies per reaction (~8 copies/µl sample input): As1, E1 (NEB) and N2 (DETECTR) targeting the Orf1ab, E- and N-gene, respectively (**Figure 1C, S1B**) (Broughton et al., 2020; Rabe & Cepko, 2020; Zhang, Ren, et al., 2020). As previously reported (Zhang, Odiwuor, et al., 2020; Zhang, Ren, et al., 2020), we observed stochastic on-off outcomes of RT-LAMP reactions with less than ~100 copies per reaction, defining 100 copies as our robust limit of detection (LoD). When tested with a diluted patient sample, the E1 (NEB) and N2 (DETECTR) primers performed best with robust detection of SARS-CoV-2 up to Cq values of ~33 (sporadic detection up to Cq 35) (**Figure S1B, Figure 2B, C**). The two corresponding amplicons overlap the Roche Cobas E-gene and the CDC-N2 RT-qPCR reference primer/probe panels, respectively, allowing direct comparisons of RT-LAMP and RT-qPCR measurements.

We next compared different DNA polymerases used for LAMP for their ability to amplify cDNA generated from synthetic SARS-CoV-2 RNA standards or patient samples. Besides Bst LF, the Large Fragment of DNA polymerase I from *Geobacillus thermophilis* used in original LAMP assays (Notomi et al., 2000), engineered Bst variants (e.g. Bst 2.0 and Bst 3.0 from NEB) have been introduced that exhibit higher salt tolerance, increased reverse transcriptase (RT) activity and increased amplification yield (Jennifer Ong, 2015). We found that the original Bst LF exhibits similar overall reaction kinetics and LoD compared to Bst 2.0 (**Figure 1D**). Although Bst LF is reported to be more salt sensitive, it allowed detection of SARS-CoV-2 from crude, inactivated patient lysate, albeit at reduced speed (**Figure S2A**). Considering the open access availability of Bst LF expression plasmids (Bhadra, Riedel, Lakhotia, Tran, & Ellington, 2020), the original Bst LF is currently the enzyme of choice for settings where engineered Bst variants are inaccessible or unaffordable.

Bst polymerases exhibit intrinsic RT activity (Shi, Shen, Niu, & Ma, 2015) and we therefore tested all three enzymes under reaction conditions lacking a dedicated RT (e.g. NEB's RTx), which is included in NEB's commercial RT-LAMP kits. Bst LF showed no RT activity in our assays (**Figure S2B**) and weak RT
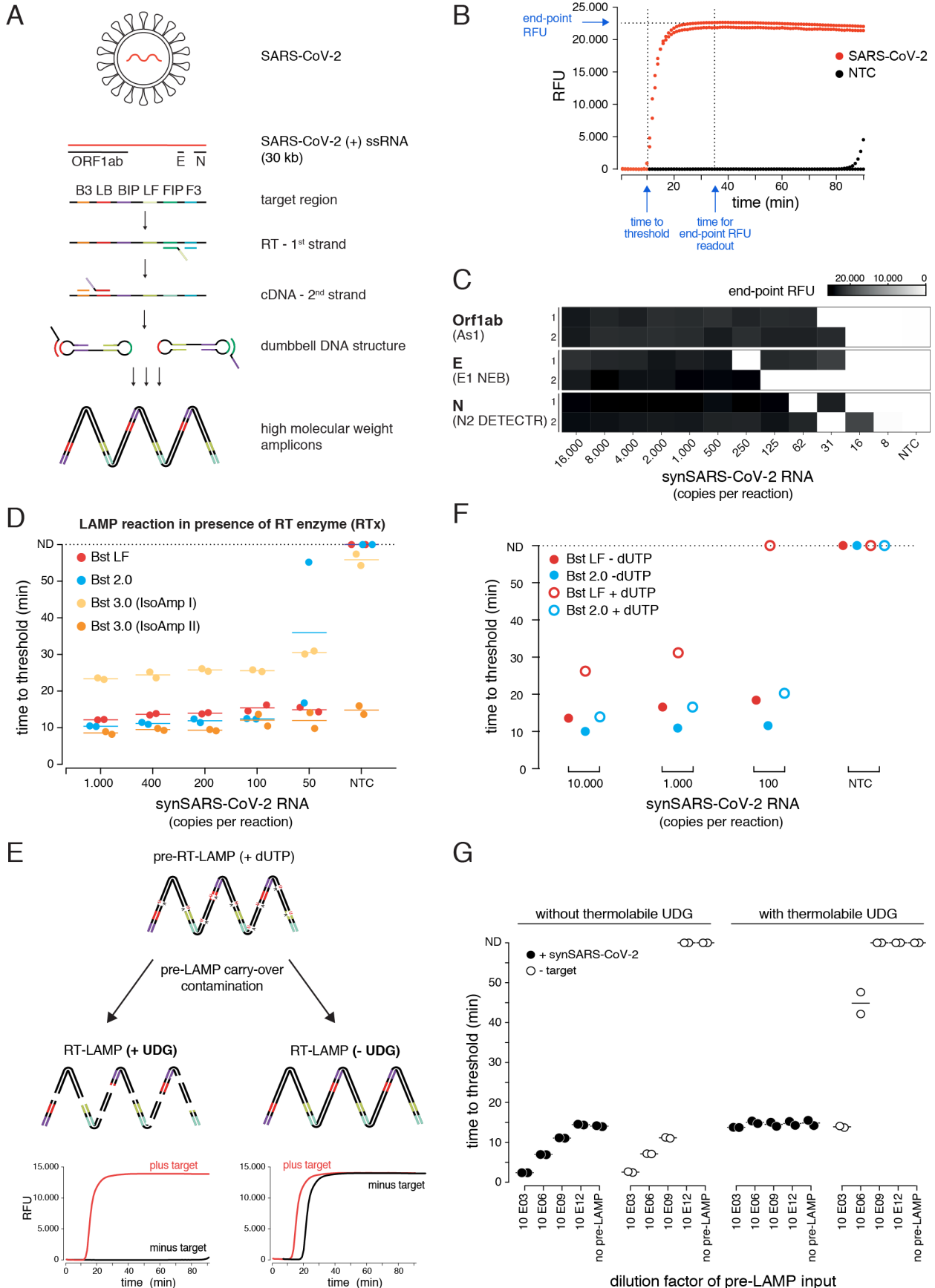
Figure 1. A sensitive, robust RT-LAMP assay with reduced carryover contamination risk. A) Schematic illustrating loop-mediated amplification (LAMP) of SARS-CoV-2 RNA and the regions targeted in this study (Orf1ab, E and N genes; depicted above). Each target region is recognized by a defined set of primers (B3, LB, BIP, LF, FIP, F3). The RNA template (red) is reverse transcribed and displaced after first-strand synthesis; the outer primer binding sites are added in the subsequent amplification step. The resulting dumbbell DNA structure acts as template for further rounds of amplification, ultimately leading to high molecular weight amplicons. **B)** Readout of a real-time fluorescence RT-LAMP reaction using 500 copies of synthetic SARS-CoV-2 (red) or water as non-targeting control (NTC, black) as input. 'Time to threshold' indicates the time at which the fluorescence value reaches threshold level (equivalent to Cq value in RT-qPCR assays), 'end-point RFU' indicates the fluorescence value after 35 minutes reaction time (used throughout this study unless indicated otherwise); RFU: relative fluorescence units. **C)** Performance of the three top primer sets for RT-LAMP-based SARS-CoV-2 detection. End-point relative fluorescence units (RFUs) of RT-LAMP reactions (in duplicates) using the indicated primer sets and serially diluted synthetic SARS-CoV-2 RNA standard as input. Water was used as no-target control (NTC). **D)** Performance (measured as 'time to threshold') of different Bst DNA polymerase variants for LAMP in combination with NEB's RTx Reverse Transcriptase on synthetic SARS-CoV-2 RNA standard. For reactions in which no amplification was recorded, 'time to threshold' is reported as 'not detected' (ND). Reactions were performed in duplicates; water was used as no-target control (NTC). **E)** Schematic depicting the principle of the dUTP/UDG system in preventing carry-over contamination. dUTP is incorporated into LAMP amplicons in a primary reaction (pre-RT-LAMP). dUTP containing LAMP products carried over into a subsequent reaction (RT-LAMP) are cleaved by UDG prior to LAMP-based amplification, making them unavailable as amplification templates. This allows robust discrimination between target and no-target control (left), which is challenged by cross-over contamination in the absence of UDG-mediated cleavage (right). **F)** Comparison of the ability of wildtype (Bst LF, red) and engineered Bst polymerase (Bst 2.0, blue) to incorporate dUTP during RT-LAMP on synthetic SARS-CoV-2 RNA standard. Reactions were either run under standard RT-LAMP conditions (-dUTP, filled circles), or supplemented with 0.7 mM dUTP, 0.7 mM dTTP and 1.4 mM of each dATP, dCTP, dGTP (open circles). Plotted is the 'time to threshold' as a measure of performance. **G)** The dUTP/UDG system minimizes cross-over contamination. Shown are performances (time to threshold) of RT-LAMP reactions in the absence (left) or presence (right) of thermolabile UDG when using synthetic SARS-CoV-2 (filled circles) or water (open circles) as input. Reactions were supplemented with the indicated dilution of a dUTP-containing pre-LAMP reaction. All reactions were performed in duplicates.

activity was observed for Bst 2.0 and Bst 3.0 when using universal Isothermal Amplification Buffer I (**Figure S2B**). In contrast, in its optimized, higher-salt buffer (Isothermal Amplification Buffer II) Bst 3.0 yielded strong yet non-specific amplification irrespective of the presence of a dedicated RT (**Figure 1D, S2B**). To ask if Bst 3.0 produced any specific amplicons under these conditions, we performed a CRISPR-Cas12 collateral cleavage assay on the Bst 3.0 LAMP products (Broughton et al., 2020). This indicated that Bst 3.0, in the absence of a dedicated RT enzyme, led to robust amplification of the synthetic standard down to 200 copies per reaction (**Figure S2C-E**). We conclude that a dedicated RT enzyme (e.g. RTx) is required for efficient and specific RT-LAMP when using Bst LF or Bst 2.0, and that reactions using Bst 3.0 alone must be carefully optimized or coupled to an additional detection step for amplicon-specific readout.

LAMP results in billion-fold amplification of target molecules. This poses a serious, rarely mentioned risk as only minor work-place or reagent contaminations with LAMP reactions can translate into large numbers of false positive assays (Kwok & Higuchi, 1989). Inspired by a previous study, we tested whether RT-LAMP based SARS-CoV-2 detection can be combined with the established contamination prevention system that utilizes dUTP and thermolabile Uracil DNA Glycosylase (Hsieh et al., 2014; Tang, Chen, & Diao, 2016). In this single-tube system, dUTP is incorporated into LAMP amplicons making them susceptible for Uracil-base cleavage in subsequent LAMP reactions that are complemented with the UDG enzyme (**Figure 1E**). Bst 2.0, but not Bst LF, showed efficient incorporation of dUTP with no loss of sensitivity or specificity (**Figure 1F**). To experimentally mimic carry-over contaminations from amplicons of prior LAMP reactions, we performed pre-RT-LAMP reactions in the

presence of dUTP, followed by dilution and addition to reactions in the presence versus absence of thermolabile UDG. Thermolabile UDG is active at room temperature yet is completely inactivated at temperatures above 50°C. In the absence of UDG, addition of a one billion-fold diluted pre-LAMP product resulted in indistinguishable signal in target vs. non-target conditions, illustrating the danger of cross-contamination. Adding UDG and a 5-minute pre-incubation step at room temperature to the RT-LAMP reaction lowered the amount of amplifiable carry-over product by more than 1.000-fold, enabling specific detection in the presence of considerable cross-over contamination product (**Figure 1G**). We conclude that the dUTP/UDG system is compatible with Bst 2.0 and that combining it with RT-LAMP reactions ensures reproducible results due to lowering the risk of false positive rates.

Having established optimal reaction conditions for RT-LAMP-based SARS-CoV-2 detection, we directly compared clinical sensitivity, using a variety of Covid-19 patient samples, of our RT-LAMP setup with gold standard one-step RT-qPCR. In a first experiment, RNA isolated from nasopharyngeal swabs or gargle lavage from Covid-19 patients served as input (**Figure 2A-C**). Using E1 or N2 primer sets for RT-LAMP, we achieved sensitive and specific detection of SARS-CoV-2 in patient samples with RT-qPCR measured Cq values of up to ~35 (~30 copies per reaction), independent of the patient sample type (**Figure 2B**). We obtained 100% positive predictive agreement rates between RT-LAMP and RT-qPCR up to Cq 33 (~100 copies per reaction) and 100% negative predictive agreement rates for qPCR negative samples (**Figure 2C**). E1 and N2 primer sets performed equally well, with a robust LoD of Cq 33-34 (**Figure 2C**). The
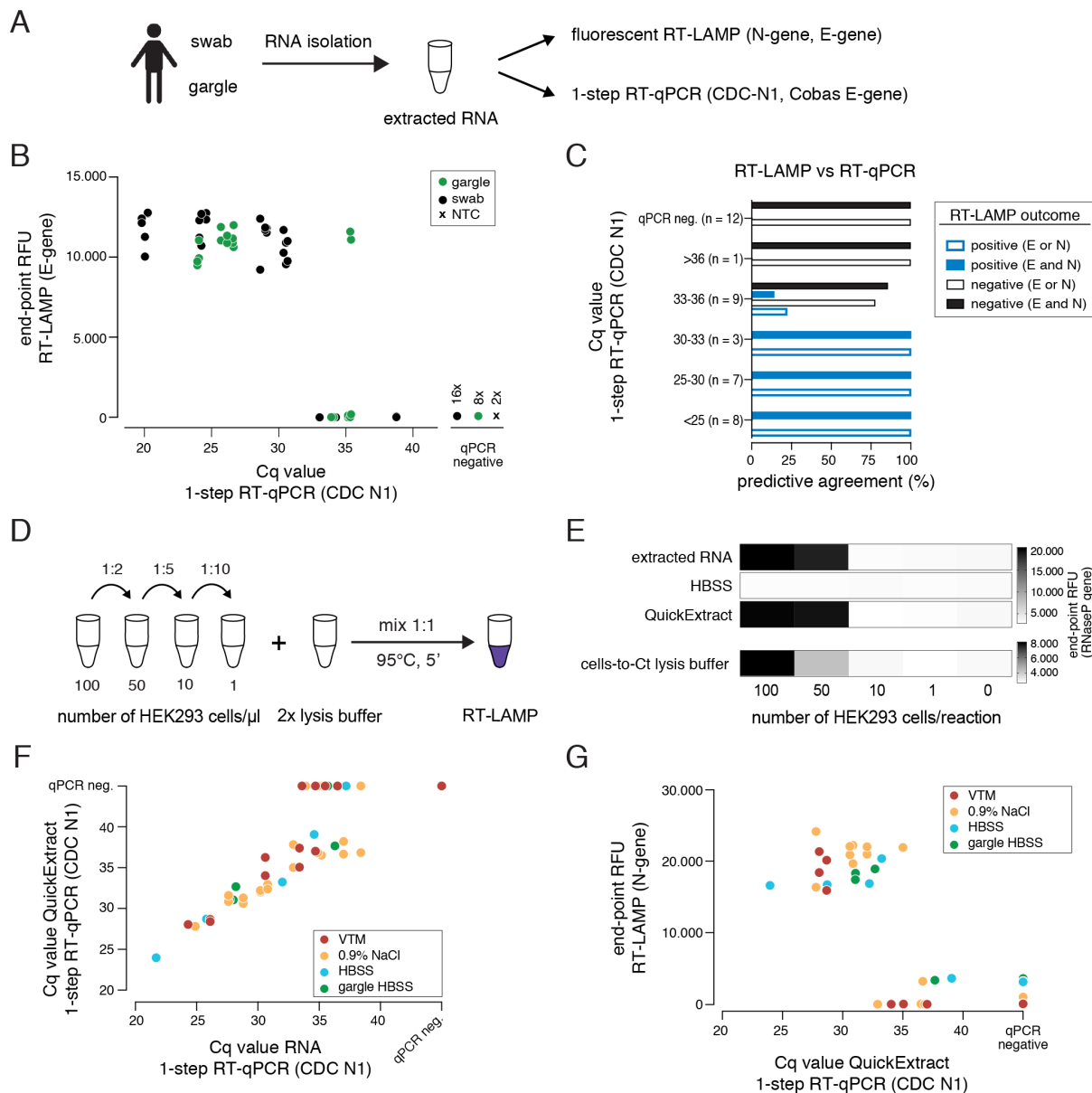
Figure 2. Robust and sensitive detection of SARS-CoV-2 from crude patient samples. A) Cartoon indicating the workflow for SARS-CoV-2 detection by either RT-LAMP or 1-step RT-qPCR from patient samples (nasopharyngeal swab or gargle) with prior RNA isolation. **B)** Comparison of RT-LAMP and RT-qPCR performance. Plotted are RT-LAMP end-point fluorescence values after 35 minutes versus the respective RT-qPCR Cq values. RNA was derived from gargle (green) or nasopharyngeal swabs (black); two no-target controls were included (black cross). Reactions in which no amplification was recorded are labelled as qPCR negative. **C)** Predictive agreement between RT-LAMP and 1-step RT-qPCR assays. Shown are percentages of positive (detected in RT-LAMP and RT-qPCR, blue bars) and negative (not detected in either RT-LAMP or RT-qPCR, black bars) predictive agreement for sample groups (defined by RT-qPCR-derived Cq values) between RT-LAMP (using E- and/or N-gene primers) and 1-step RT-qPCR. **D)** Cartoon indicating the workflow for testing different crude sample preparation methods using HEK293 cells as input. **E)** Performance of different crude sample preparation methods in RT-LAMP. Shown are end-point relative fluorescence units (RFUs) for RT-LAMP reactions targeting human RNAseP on sample inputs derived from defined numbers of HEK293 cells mixed 1:1 with indicated 2x buffers (workflow as in D; extracted RNA served as a positive control). **F)** Comparison of QuickExtract crude sample input versus extracted RNA as input using 1-step RT-qPCR. Covid-19 patient nasopharyngeal swabs or gargle samples (color coded according to the indicated collection medium) were either processed with the QuickExtract workflow (crude sample input) or RNA was extracted using an automated King Fisher RNA bead purification protocol. Reactions in which no amplification was recorded are labelled as qPCR negative. **G)** Performance of RT-LAMP with QuickExtract treated crude Covid-19 patient sample input (same samples as in F). Depicted is the correlation of Cq values from RT-qPCR performed on QuickExtract treated samples versus corresponding end-point relative fluorescence units (RFUs) from RT-LAMP reactions.

availability of several equally well-performing primer sets increases the robustness of the assay as it will reduce the number of possible false negatives caused by suboptimal sample quality or by mutations in the viral genome coinciding with primer binding sites (Artesi et al., 2020).

5

A major bottleneck in FDA-approved RT-qPCR-based SARS-CoV-2 nucleic acid detection assays is their dependence on time-consuming and expensive RNA purification from patient samples. Inspired by recent findings that the RNA purification step can be circumvented (Ladha, Joung, Abudayyeh, Gootenberg, & Zhang, 2020; Rabe & Cepko, 2020), we assessed different direct sample input/lysis conditions for their compatibility with sensitive RT-LAMP. Besides simple heat inactivation, we tested two previously published lysis and sample inactivation buffers, namely QuickExtract (Lucigen) (Ladha et al., 2020) and the 'Cells-to-Ct' lysis buffer (Joung et al., 2017). As a first assessment of different lysis conditions, we compared crude lysates from serially diluted HEK293 cells to isolated RNA from equivalent numbers of cells as input for RT-LAMP reactions targeting the human reference gene RNase P subunit 30 (**Figure 2D, E**). In agreement with prior findings (Ladha et al., 2020), a five-minute incubation of patient samples with QuickExtract at 95°C performed equally well compared to a standard Trizol RNA extraction step (**Figure 2E**). Follow-up experiments substantiated the exceptional ability of QuickExtract, in combination with heat treatment, to preserve RNA even under conditions where exogenous RNase A was added (**Figure S3**).

To benchmark QuickExtract solution on Covid-19 patient samples, we performed RT-qPCR on either purified patient RNA or crude QuickExtract lysate. Irrespective of the sample type (swab or gargle), we observed a strong agreement between the corresponding RT-qPCR measurements (**Figure 2F**). Only samples with very low viral titres (high Cq values) became undetectable in the QuickExtract samples, presumably as ~20-fold less patient material equivalent was used compared to reactions using isolated RNA as input (**Figure 2F**). Importantly, RT-LAMP performed equally well to extracted RNA when using QuickExtract crude sample input across different transport media and different sample types (swabs in viral transport medium (VTM), swabs in 0.9% NaCl, swabs or gargle in HBSS buffer), with a limit of RT-qPCR-measured Cq values of 33 (~100 copies) and identical predictive performance rates (**Figure 2G**). No false positives were observed, demonstrating the high specificity and sensitivity of RT-LAMP on crude samples lysed and inactivated with QuickExtract solution. Heat inactivation with QuickExtract is therefore a robust, rapid and simple method to prepare patient samples for SARS-CoV-2 testing using RT-LAMP.

In our previous experiments, we used real-time fluorescence based on an intercalating DNA dye to read RT-LAMP-based target gene amplification. Given its dependency on specialized equipment, this detection method is prohibitive for low-resource settings or home-testing. Colorimetric detection systems resulting in a visual color change upon target DNA amplification provide an attractive low-cost alternative to fluorescence detection (**Figure 3**) (Goto, Honda, Ogura, Nomoto, & Hanaki, 2009; Tanner, Zhang, & Evans, 2015). Two colorimetric concepts are compatible with RT-LAMP: First, pH dependent dye indicators such as Phenol Red induce a color change from pink to yellow when the pH value of the reaction decreases upon DNA amplification (Tanner et al., 2015). Due to its pronounced color change, this is the most commonly used readout for RT-LAMP assays. Alternatively, metal ion indicators such as Hydroxynaptholblue (HNB) induce a color change from purple to blue upon a drop in free Mg^{2+} ions, which form a Mg-pyrophosphate precipitate upon DNA amplification (**Figure 3A**) (Goto et al., 2009).

Both colorimetric assays were as sensitive as the fluorescent readout (which could be performed in the same reaction tubes by adding fluorescent dye) in our RT-LAMP setup when using synthetic SARS-CoV-2 standard in water as input (**Figure 3B, S4**). However, when using crude QuickExtract lysate as input, the pH dependent readout failed entirely or was inconclusive despite RT-LAMP amplifying the target as evidenced by the fluorescent readout (**Figure 3C, S4**). In contrast, the HNB-dependent color change was not affected by QuickExtract solution, even when mixed with various sample buffers such as VTM, NaCl or HBSS (**Figure 3C**). We suspect that the QuickExtract solution is strongly buffered thereby preventing the required pH change that is typically generated during LAMP.

When tested in a clinical setting, RT-LAMP coupled to the HNB readout enabled us to robustly detect SARS-CoV-2 in patient samples with RT-qPCR values of up to ~34 (corresponding to ~50 copies per reaction of reference standard) with no false positives and 100% positive predictive agreement up to Cq 33 (~100 copies per reaction) (**Figure 3D, E, S4A**). The detection outcome was independent of the sample type, and we successfully used QuickExtract lysate from nasopharyngeal swabs, gargle solution or sputum samples (**Figure 3D, S4B**). We conclude that HNB is the superior colorimetric detection assay for RT-LAMP with QuickExtract or other strongly buffered crude sample inputs as it allows performing the RT and LAMP amplification reactions under ideal buffer conditions.

To accurately determine the sensitivity threshold of HNB RT-LAMP, we generated a systematic dilution series of a positive Covid-19 patient sample in QuickExtract and used absorbance at 650 nm in a microplate reader to unambiguously determine the color change (Goto et al., 2009). We tested all dilutions by RT-qPCR and HNB RT-LAMP in parallel (**Figure 3F, G**). For this experiment, HNB RT-LAMP was performed by incubating microtitre plates containing the individual reactions in a simple, temperature-controlled oven. When considering samples with 650 nm absorbance values higher than for any co-measured negative control, HNB RT-LAMP allowed specific detection up Cq 34.9 with no false positives (**Figure 3F, G**). We conclude that, while read-out by fluorescence is the method of choice for high-throughput settings due to the higher dynamic range, direct absorbance measurement of the HNB-induced color change offers an attractive alternative, semi-quantitative readout for large numbers of RT-LAMP reactions performed in parallel.

Even under optimized conditions, RT-LAMP exhibits a limit of robust detection at around 50 viral RNA molecules per reaction (corresponding to Cq values of
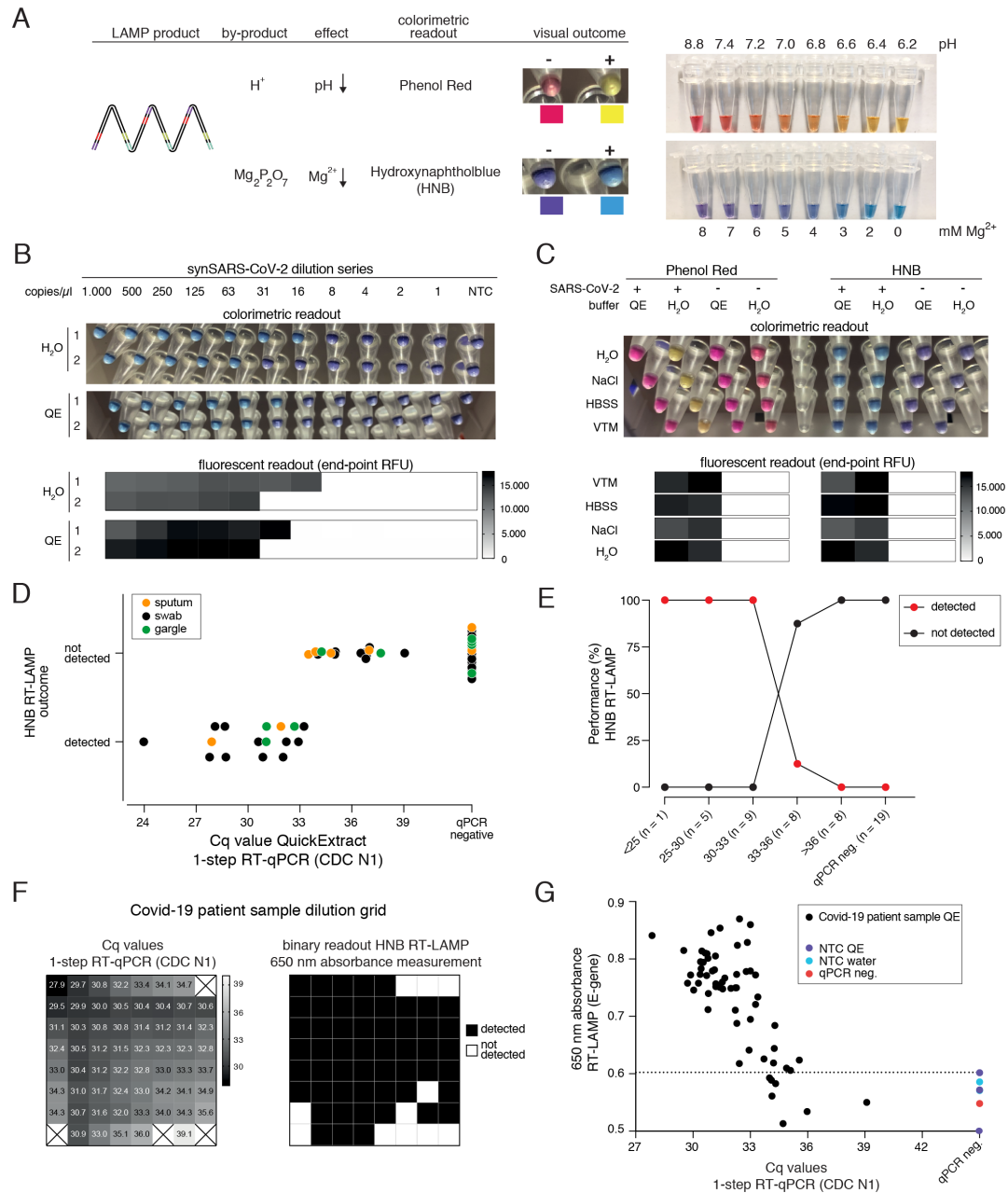
Figure 3. HNB RT-LAMP enables colorimetric SARS-CoV-2 detection from crude patient samples. A) Schematic illustrating the properties of pH-sensitive (Phenol Red, top) and Mg^{2+} concentration sensitive (Hydroxynaphtholblue, HNB, bottom) colorimetric readouts for LAMP. Phenol Red interacts with protons (H^+) generated during DNA amplification, which causes a color change from pink/red to yellow (right: the color range of the Phenol Red-containing colorimetric RT-LAMP mastermix (NEB) at relevant pH values). Magnesium pyrophosphate precipitate produced during DNA amplification lowers the free Mg^{2+} concentration, causing a color change of the HNB dye from purple to sky-blue (right: the color range of solutions with HNB at relevant Mg^{2+} concentrations). **B)** Influence of QuickExtract on HNB RT-LAMP performance. Shown is the colorimetric HNB readout of RT-LAMP reactions (after 35 minutes; in duplicates) using indicated copy numbers of SARS-CoV-2 RNA standard in water or QuickExtract and the corresponding co-measured end-point fluorescence values (heatmaps are shown below). **C)** QuickExtract lysis buffer is compatible with HNB colorimetric readout but incompatible with Phenol Red colorimetric readout of RT-LAMP reactions. Shown are RT-LAMP reaction outcomes (upper panel: colorimetric readout after 35 minutes, lower panel: fluorescent end-point values) when using 500 copies of synthetic SARS-CoV-2 RNA standard in indicated sample media diluted 1:1 with water or 2x QuickExtract solution as input. **D)** HNB RT-LAMP performance on Covid-19 patient samples lysed in QuickExtract solution. Shown is the binary colorimetric HNB readout of RT-LAMP reactions (N gene) using indicated patient samples (sputum (orange), swab (black), gargle (green)) plotted against the corresponding Cq values from RT-qPCR. **E)** Predictive agreement between HNB RT-LAMP and RT-qPCR assays using patient samples lysed in QuickExtract solution. Samples were grouped according to their RT-qPCR Cq values, and the percentage of detected (red) and not detected (black) samples (based on HNB RT-LAMP) of the total number of samples per group was plotted. **F)** Schematic illustrating the serial dilution grid of a Covid-19 positive patient sample (Cq of 28) in QuickExtract. The heatmap (left) indicates Cq values determined by 1-step RT-qPCR (values above Cq 40 are indicated by black crosses). The grid (right) indicates the binary read-out (black: detected; white: not detected) of HNB RT-LAMP as measured by 650 nm absorbance). **G)** Scatterplot showing HNB RT-LAMP performance (measured by 650 nm absorbance) versus qPCR-determined Cq values on the serial dilution grid shown in F, including no-target controls (NTC; purple: in QuickExtract (QE), blue: in water) and a Covid-19-negative patient sample (qPCR negative, red). Horizontal dashed line indicates the maximum absorbance obtained for any negative control (y = 0.602).
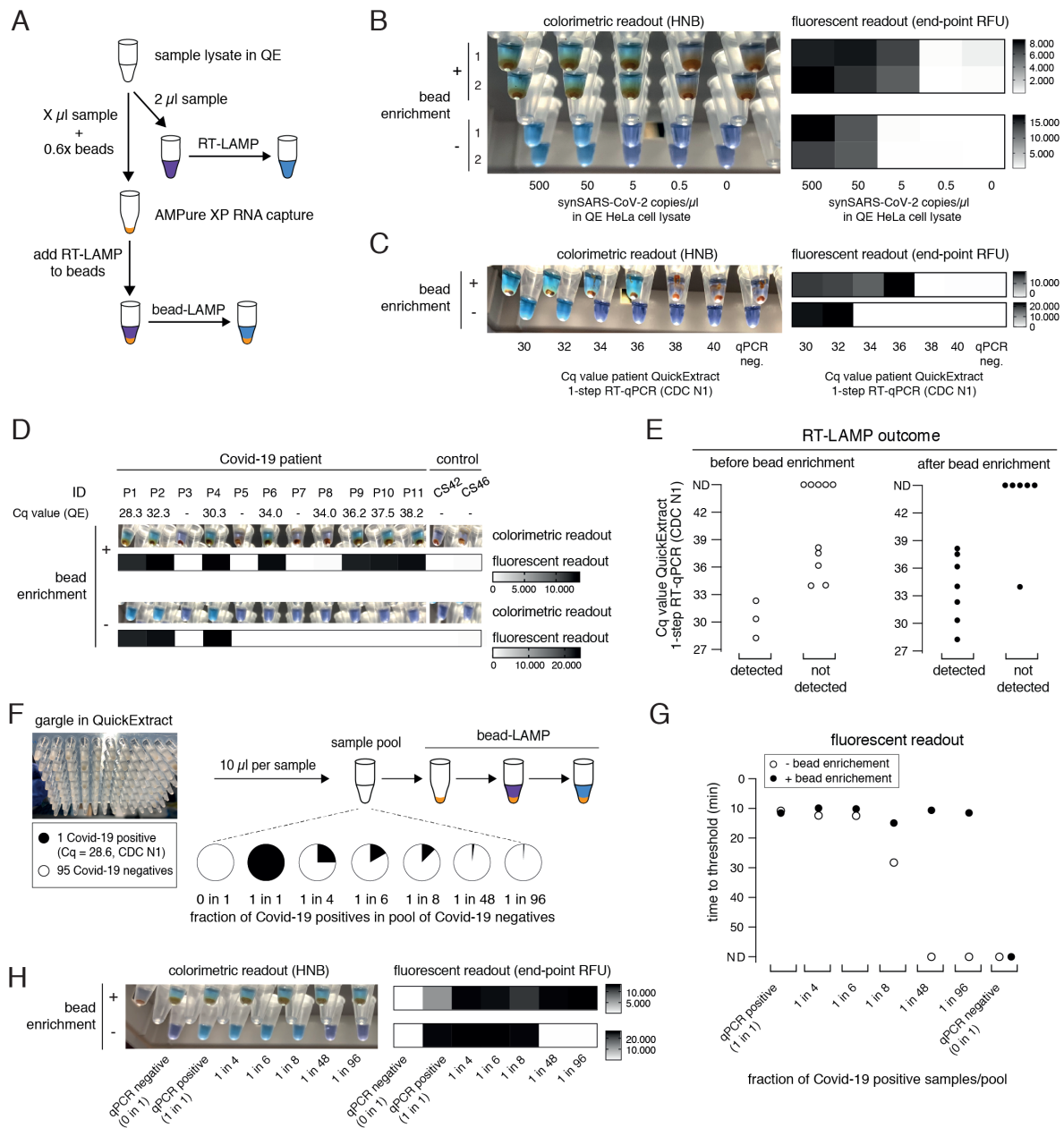
Figure 4. bead-LAMP increases sensitivity of RT-LAMP assays. A) Schematic illustrating the bead-LAMP workflow in comparison to the regular RT-LAMP workflow. Volumes of sample lysate in QuickExtract (QE) as used in the experiments shown in B-E are indicated. AMPure XP RNA capture beads were used at 0.6x of the volume of the sample lysate (0.6x beads). **B)** Performance of bead-LAMP using a synthetic SARS-CoV-2 RNA standard spiked-in at the indicated concentration into HeLa cell QuickExtract (QE) lysate. The image (left) shows HNB end-point colorimetric readout of RT-LAMP reactions and the heatmap (right) shows co-measured end-point relative fluorescence units (RFUs), with or without prior bead enrichment. All reactions were performed in duplicates. **C)** Performance of bead-LAMP on crude patient samples. The image (left) shows HNB end-point colorimetric readout and the heatmap (right) shows co-measured end-point relative fluorescence units (RFUs) of RT-LAMP on serially diluted patient samples in QuickExtract-prepared HeLa cell lysate, with or without prior bead enrichment. Cq values are estimated based on RT-qPCR measurement of the Cq value of the undiluted parental Covid-19 patient sample prior to bead enrichment. All reactions were performed in duplicates. **D)** Performance of bead-LAMP on a Covid-19 positive panel of patient samples in QuickExtract. The images depict the HNB colorimetric end-point readout, and the heatmaps underneath show co-measured end-point relative fluorescence units (RFUs) of RT-LAMP reactions, with or without prior bead enrichment, using 8 Covid-19-positive and 5 negative samples as input (P1-P11, Covid-19 patient sample; CS42 and CS46, healthy controls). Corresponding Cq values were obtained by measuring the same QuickExtract (QE) patient samples by 1-step RT-qPCR prior to bead enrichment. **E)** Bead enrichment increases the sensitivity of RT-LAMP. Patient samples from D) were classified as detected or not detected based on the HNB RT-LAMP assay before (left, open circles) and after (right, filled circles) bead enrichment and plotted against their respective Cq values obtained from QuickExtract (QE) RT-qPCR (Cq values for qPCR negative samples are labelled as not detected, ND). **F)** Schematic illustrating the pooled testing strategy using bead-LAMP. A single Covid-19 positive patient gargle sample in QuickExtract (Cq ~28; black) was mixed with different amounts of 95 pooled SARS-CoV-2 negative samples (all in QuickExtract; white) yielding seven sample pools with indicated ratios of positive to negative samples. **G)** Shown is the performance (measured as time to threshold) of bead-LAMP (filled circles) compared to regular RT-LAMP (open circles) on the patient pools defined in F. ND = not detected within 60 minutes of RT-LAMP incubation. **H)** Images showing the endpoint HNB colorimetric readout (left) and fluorescent readout (endpoint RFU; right) of samples measured in G) with or without prior bead enrichment.

8

~34). As only a small amount (in our case 2 μl) of the patient sample lysed in QuickExtract is used per LAMP reaction, we set out to establish an RNA pre-enrichment step to increase the assay sensitivity. We took advantage of carboxylated magnetic beads to enrich RNA from a larger volume of QuickExtract lysates on the bead surface in the presence of crowding agents and salt (Hawkins, O'Connor-Morin, Roy, & Santillan, 1994). We then reasoned that, instead of eluting RNA from the beads, adding the RT-LAMP mix directly to the beads should maximize the number of viral RNA molecules per reaction by orders of magnitude, depending on the sample input volume (in our case up to 50-fold) (**Figure 4A**). We tested this approach, termed bead-LAMP, by using either bead-enriched or non-enriched synthetic SARS-CoV-2 RNA in HeLa cell QuickExtract lysate as RT-LAMP input. Indeed, bead-LAMP using 60 μl QuickExtract lysate as input displayed an at least ten-fold increased sensitivity, corresponding to a LoD of ~10 copies per reaction (**Figure 4B**). The fluorescence readout of the LAMP reaction exhibited overall lower values yet similar kinetics (**Figure S6B**), indicating that bead-LAMP is compatible with real-time kinetic analysis alongside colorimetric end-point detection (**Figure 4B**). After bead enrichment the recovery rates of synthetic SARS-CoV-2 RNA determined by RT-qPCR ranged from 68-98%, showing the high efficiency of the approach (**Figure S5**).

We next tested bead-LAMP on a dilution series of a Covid-19 patient sample in QuickExtract (Cq of ~30) and observed a similar ten-fold increased sensitivity, corresponding to a LoD of up to Cq 37 in patient samples (**Figure 4C**). When performing bead-LAMP on individual Covid-19 patient samples, we found a dramatic improvement in the diagnostic performance. With the exception of one patient that we were not able to detect via RT-LAMP for unknown reasons, all qPCR positive samples (with Cq values up to ~38) were identified while no qPCR negative sample was detected (**Figure 4D, E**).

The boost in sensitivity opened the door for establishing a pooled RT-LAMP testing strategy. We mixed one crude Covid-19 positive patient gargle sample in QuickExtract (N1-CDC RT-qPCR Cq ~28) with different volumes of a pool of 95 crude SARS-CoV-2 negative gargle samples in QuickExtract (**Figure 4F, S6A**). Each pool was tested by standard RT-LAMP and bead-LAMP. Without bead enrichment, pools with at least 12.5% (1 out of 8) of Covid-19 positive sample were identified. In contrast, bead-LAMP enabled detection of all pools containing SARS-CoV-2, even the pool containing just 1% (1 out of 96) of Covid-19 positive sample (**Figure 4G, H, S6B**). An independent experiment, in which we tested bead-LAMP on a dilution series of a Covid-19 positive patient of Cq ~30 in QuickExtract HeLa cell lysate, led to a similar conclusion: again, the pool containing only ~1% of the Covid-19 positive sample was detectable only with prior bead enrichment (**Figure S6C-E**). With merely 21 reactions (one entire 96-well plate pool, eight column pools, twelve row pools), a single positive patient of Cq ~30 can thus be detected amongst hundred individuals. We conclude that a cheap, fast (~5-10 minutes) and simple pre-enrichment step boosts the sensitivity of RT-

LAMP at least ten-fold, making this approach highly attractive and robust for pooled testing strategies.

The lack of specialized laboratory equipment, such as precision pipettes or temperature-controlled incubators, presents a major obstacle for the implementation of SARS-CoV-2 detection in most environments, including home settings. We therefore explored approaches to adapt the HNB RT-LAMP protocol to low-resource settings. In order to make RT-LAMP independent of pipettes, we adopted a previously reported strategy for sample clean-up and transfer using filter paper (Y. Zou et al., 2017). Using a sample transfer method based on Whatman filter paper dipsticks (**Figure 5A**), we reliably detected SARS-CoV-2 RNA from Covid-19 patients with moderate viral titres (Cq ~27) (**Figure 5B**). Importantly, we found that introducing a wash step with 130 mM sodium chloride solution increased the sensitivity and enabled detection of SARS-CoV-2 from patient samples with Cq values ~32, mimicking the sensitivity of standard RT-LAMP assays (**Figure 5B**).

Due to their isothermal nature, RT-LAMP reactions require stable incubation temperatures ~62-63°C. This can be provided using equipment ranging from high end instruments to the most basal setup where boiling and room temperature water are mixed at a defined ratio. We tested a commercially available sous-vide heater to create a temperature-controlled reaction environment (water bath) for home-based testing (**Figure 5C**). When combined with the filter paper-based sample clean-up and transfer method, this setup, termed HomeDip-LAMP, was able to accurately detect, within 35 minutes, two out of two viral genes in a Covid-19-positive patient gargle sample without false positives among Covid-19 negative gargle samples (**Figure 5D**). Detection accuracy and reaction speed matched HNB RT-LAMP reactions with pipetted sample input and laboratory equipment (**Figure 5D**). Taken together, our findings provide a basis for the development of a simple SARS-CoV-2 detection platform, which can be implemented in any low-tech environment.

Discussion

RT-LAMP is an in-expensive, specific nucleic acid detection assay that provides test results in less than 30 minutes. Its independence of specialized laboratory equipment makes it highly attractive for settings with limited resources or for population-scale testing. RT-LAMP's benefits over other nucleic acid detection methods are further elevated by its compatibility with colorimetric visual readouts and with patient sample input protocols that circumvent an extra RNA extraction step. These recent innovations, however, present drawbacks for sensitive and robust nucleic acid diagnostics. Here we provide strategies to overcome these obstacles and introduce rapid, highly sensitive, and simplified RT-LAMP assays that hold the promise to contribute towards effective containment of the current SARS-CoV-2 pandemic.
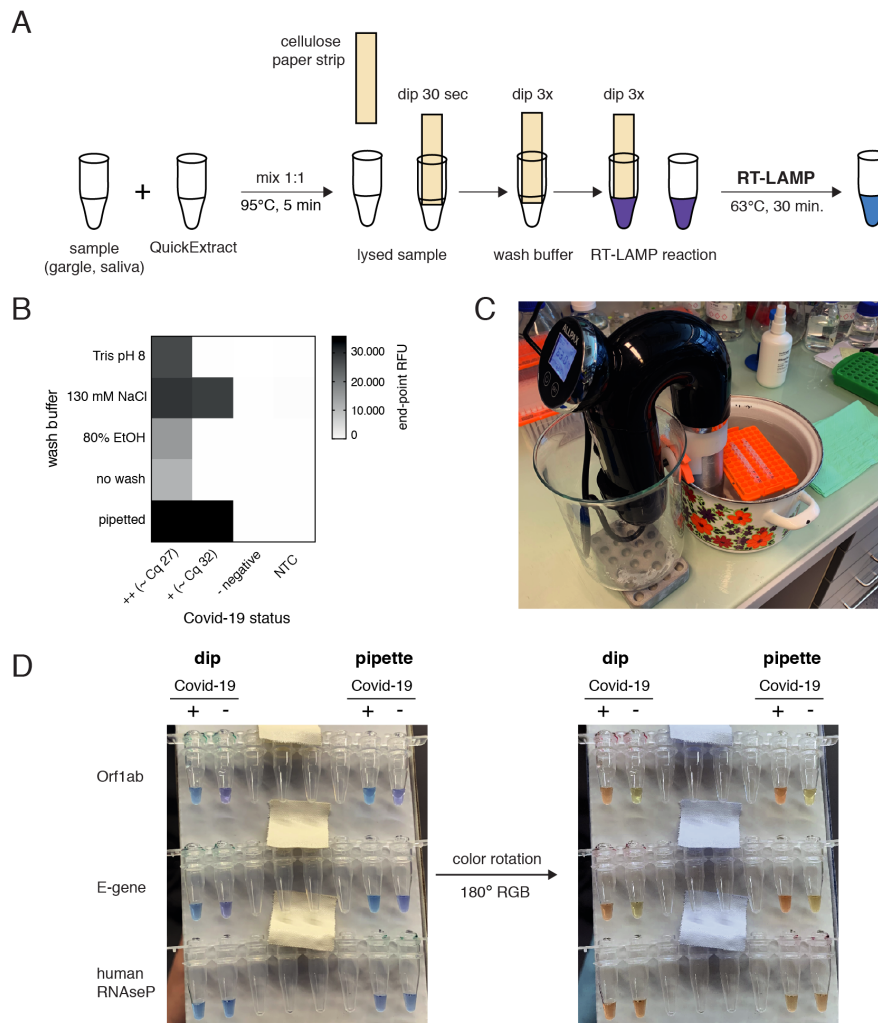
Figure 5. HomeDip-LAMP enables SARS-CoV-2 detection in low-resource and home settings. A) Schematic depicting the HomeDip-LAMP workflow. Samples are mixed 1:1 with QuickExtract lysis buffer and inactivated at 95°C for 5 minutes. Cellulose paper dipsticks are loaded by dipping into the crude sample for 30 seconds. After a brief washing step (3x dipping into wash buffer), RNA is released into pre-distributed RT-LAMP reaction mixes by 3x dipping. RT-LAMP reactions are performed in a water bath at 63°C and read out after 35 minutes. **B)** Influence of different wash conditions on SARS-CoV-2 detection using RT-LAMP with paper dipstick sample transfer. Heatmap showing end-point relative fluorescence units (RFUs) at 30 minutes of RT-LAMP reactions after transferring 2 µl of high titre (++, Cq ~27), medium-to-low titre (+, Cq. ~32) or negative Covid-19 patient samples in QuickExtract into 8 µl of RT-LAMP reaction mix using cellulose paper dipsticks. Dipsticks were washed in between in indicated solutions or transferred without washing. A sample series where 2 µl were transferred by pipetting ('pipette') is shown alongside (NTC = no target control). **C)** Image showing the water bath setup with a sous-vide heater (black) for HomeDip-LAMP. Reaction tubes were kept upright and submerged using floating plastic pipette tip racks (orange). **D)** Detection of SARS-CoV-2 using HomeDip-LAMP. Left image shows true color readout (HNB dye) of HomeDip-LAMP (left 2 tubes) and pipetted LAMP (right 2 tubes) reactions using a Covid-19-positive (+) and -negative (-) patient sample in QuickExtract as input (30 minute end-point; water bath incubation at 63°C). Amplicons are indicated to the left; the human RNAseP amplicon served as positive control. The image to the right shows a color-rotated (180° in RGB space) readout of the left images for easier readout.

The specificity of a diagnostic test is determined by the false positive rate. Especially in nucleic acid diagnostics, which is based on target amplification, simple carry-over cross-contamination can pose serious challenges. In this respect, LAMP is particularly challenging due to its enormous level of target amplification. Especially in laboratory environments where large numbers of samples are tested with a common set of primers, this can lead to a considerable false positive rate. Similarly challenging are RT-LAMP setups that require opening of the reaction vessels for downstream analyses (Broughton et al., 2020). We demonstrate that the established dUTP/thermolabile UDG system is fully compatible with LAMP workflows and lowers the risk for contamination by at least 1.000-fold without compromising specificity or sensitivity of SARS-CoV-2 detection (**Figure 1**). We propose adding the dUTP/UDG system to RT-LAMP reactions as it considerably lowers the risk of false diagnoses, irrespective of the setup.

Certified SARS-CoV-2 diagnostic workflows include an expensive and lengthy RNA isolation step. To circumvent this problem, several crude sample

inactivation protocols have been developed that are compatible with direct downstream reverse transcription and amplification steps. While these advancements have simplified SARS-CoV-2 detection considerably, the required buffered solutions or reducing agents present a challenge for the commonly used pH indicator-based colorimetric LAMP readout. For example, strongly buffered lysis solutions such as QuickExtract are not compatible with Phenol dye detection, resulting in substantial false negative rates. Similarly, false positives have been reported for patient sample types with acidic pH such as saliva (Lalli et al., 2020). We employed the known metal indicator Hydroxynaptholblue (HNB) as a robust alternative for colorimetric detection of SARS-CoV-2 with no false positives or false negatives detected with any tested sample buffer (**Figure 3, S4**). HNB RT-LAMP is a highly robust and stream-lined assay and thus suited for diagnostic efforts in home settings.

A major drawback of using patient samples directly for nucleic acid diagnostics is the resulting drop in sensitivity. While an upstream RNA isolation step allows the concentration of viral template molecules, this is not the case for crude extraction methods. With a robust LoD of ~50-100 copies per reaction, RT-LAMP with crude patient sample input can only detect medium to high viral titres. Our development of bead-LAMP, a simple RNA enrichment protocol with magnetic beads, sets the stage for highly sensitive SARS-CoV-2 detection in samples from individual patients or patient pools (**Figure 4**). While similar to a recently reported protocol based on silica particles (Rabe&Cepko), our approach depends only on a magnet and adds just 5-10 minutes to the standard protocol. Bead-LAMP does not require centrifugation and can be performed manually with a simple magnet, an automated magnetic particle processor like the KingFisher or on fully automated liquid handling platforms. It is especially suited for mass-scale pathogen surveillance via sample pooling strategies. Combined with the HNB colorimetric read-out, bead-LAMP allows for screening hundreds of individuals in pooled reactions in simple PCR strips. Bead-LAMP is also an attractive alternative to ultra-sensitive RT-qPCR when used on single patient samples. For example, return-to-work policies after infection typically require two consecutive negative tests where the detection limit of standard RT-LAMP is likely not sufficient.

To illustrate the practical implications of diagnostic sensitivity, we used our clinical RT-qPCR tests from nasopharyngeal swabs to calculate viral copies per entire clinical sample as done in (Wölfel et al., 2020). **Figure S7A** shows that the viral titer per sample ranges from ~650 to 2×10^8 viral RNA copies. Grouping patient samples according to their ability to infect cells in culture ($>10^6$ viral copies per swab) (Wölfel et al., 2020) further allows to separate them roughly into infectious and non-infectious groups. RNA isolation coupled to RT-qPCR is able to detect this enormous range of viral titers (5 copies per reaction) (Corman et al., 2020). Without distinguishing between infectious or non-infectious individuals, RT-LAMP on purified RNA (LoD: 100 copies per reaction for RT-LAMP) would detect ~ 80% of all infected individuals (**Figure S7B**).

RT-LAMP on QuickExtract lysate directly prepared from crude sample lowers the number of detectable individuals to 64% or 50% when swab volumes of 0.5 ml or 3 ml are used, respectively. In contrast, the theoretical detection rate of bead-LAMP is ~92% relative to RT-qPCR on extracted RNA, when considering 100% RNA recovery on beads, and up to 86% when taking the average 77% recovery measured with our protocol (**Figure S5**) into account. Of note, bead-LAMP is more sensitive than RT-qPCR performed on crude QuickExtract lysate, which detects ~80% of infected individuals in our experiments. Importantly, infectious patients are identified at 100% detection rate in all RT-LAMP detection formats, highlighting the relevance of RT-LAMP for clinical diagnostics and population screening. Taken together, in combination with minimizing sample volumes of nasopharyngeal swabs, bead-LAMP, without a dedicated RNA purification step, has diagnostic sensitivity that is currently defined by gold-standard certified RT-qPCR assays. At the same time, bead-LAMP outperforms RT-qPCR in terms of speed, cost (~1.5 USD for commercial QuickExtract & RT-LAMP reagents plus 0.1 – 0.25 USD for commercial magnetic beads per reaction), and comparatively low equipment needs.

While bead-LAMP enables pooled testing, particularly in laboratory settings, reliable and sensitive home-tests provide important alternative strategies in controlling and ending the Covid-19 pandemic (Taipale, Romer, & Linnarsson, 2020). Towards this end, we present a simple strategy for sample RNA binding and transfer using cellulose paper strips. With HomeDip-LAMP, SARS-CoV-2 detection can be performed in home settings without the use of pipettes (**Figure 5**). Only sample inactivation buffer, paper-strips, wash and reaction solution together with a stable heat-source such as a water bath are required. We envision that a combination of bead-LAMP with HomeDip-LAMP could be adapted for ultra-sensitive home testing. In such a combined approach, beads could be added to the inactivated sample, followed by binding to a magnetic rod and dipping as described for cellulose paper strips.

In summary, our improvements over existing RT-LAMP workflows enable robust, in-expensive and ultra-sensitive detection of SARS-CoV-2 and should also be applicable to other pathogens. There are, however, several remaining challenges, especially with respect to the world-wide distribution and access to RT-LAMP reagents. All of our assays were performed with commercial reagents that require -20°C storage, which is prohibitive for low-resource settings. Also, pre-aliquoted ready-to-use reaction mixes required for home-testing may be less stable even when stored at low temperature. Lyophilisation of the reaction mix or addition of protein stabilizing chemicals such as Trehalose might ameliorate those (Jain & Roy, 2010). The most significant limitation for SARS-CoV-2 testing in developing countries, however, is reagent availability. Our data indicate that Bst 2.0, in combination with RTx Reverse Transcriptase, shows superior performance over the original Bst LF in terms of reaction speed, assay sensitivity and dUTP incorporation efficiency. Bst 2.0

and RTx enzymes are engineered and proprietary enzymes. The open access sharing of expression plasmids for on-site production is therefore not possible. Efforts from research laboratories and the business sector are required to overcome socio-economic barriers preventing open reagent access by enabling the local production and distribution of RT-LAMP reagents, especially in developing countries. Combating the Covid-19 pandemic will require access to diagnostic tests in all countries ("The COVID-19 testing debacle," 2020). Our improvements of the RT-LAMP workflow provide a clear path forward to moving towards testing for everyone.

Acknowledgements

Author contributions

MJK, JJR and JS designed, performed and analyzed all experiments; MPSD, RFP and RH processed patient samples; MT, TS, AZ, MF and CW provided patient samples; JZ, MF and CW coordinated clinical validation studies; JZ acquired project funding; NAT provided important information on LAMP technology; the VCDI enabled and supported Covid-19 testing initiatives at the Vienna BioCenter; MJK, AP and JB conceived the project; AP and JB coordinated and supervised the project; MJK, with the help of JJR, JS, AP and JB wrote the paper.

Funding

Competing interests

NAT is employee and stockholder of New England Biolabs, the manufacturer of reagents used in the study. All other authors declare no conflict of interest.

References

Anahtar, M. N., McGrath, G. E. G., Rabe, B. A., Tanner, N. A., White, B. A., Lennerz, J. K. M., . . . Rosenberg, E. S. (2020). Clinical assessment and validation of a rapid and sensitive SARS-CoV-2 test using reverse-transcription loop-mediated isothermal amplification. *medRxiv*, 2020.2005.2012.20095638. doi:10.1101/2020.05.12.20095638

Artesi, M., Bontems, S., Gobbels, P., Franckh, M., Boreux, R., Meex, C., . . . Durkin, K. (2020). Failure of the cobas® SARS-CoV-2 (Roche) E-gene assay is associated with a C-to-T transition at position 26340 of the SARS-CoV-2 genome. *medRxiv*, 2020.2004.2028.20083337. doi:10.1101/2020.04.28.20083337

Bhadra, S., Riedel, T. E., Lakhotia, S., Tran, N. D., & Ellington, A. D. (2020). High-surety isothermal amplification and detection of SARS-CoV-2, including with crude enzymes. *bioRxiv*, 2020.2004.2013.039941. doi:10.1101/2020.04.13.039941

Broughton, J. P., Deng, X., Yu, G., Fasching, C. L., Servellita, V., Singh, J., . . . Chiu, C. Y. (2020). CRISPR–Cas12-based detection of SARS-CoV-2. *Nat Biotechnol*. doi:10.1038/s41587-020-0513-4

Butler, D. J., Mozsary, C., Meydan, C., Danko, D., Foox, J., Rosiene, J., . . . Mason, C. E. (2020). Shotgun Transcriptome and Isothermal Profiling of SARS-CoV-2 Infection Reveals Unique Host Responses, Viral Diversification, and Drug Interactions. *bioRxiv*, 2020.2004.2020.048066. doi:10.1101/2020.04.20.048066

CDC, U. (2020). Centers for Disease Control and Prevention. Real-time RT–PCR Panel for Detection 2019-nCoV. Retrieved from https://www.cdc.gov/coronavirus/2019-ncov/lab/rt-pcr-detection-instructions.html

Corman, V. M., Landt, O., Kaiser, M., Molenkamp, R., Meijer, A., Chu, D. K., . . . Drosten, C. (2020). Detection of 2019 novel coronavirus (2019-nCoV) by real-time RT-PCR. *Euro surveillance : bulletin Europeen sur les maladies transmissibles = European communicable disease bulletin, 25*(3), 2000045. doi:10.2807/1560-7917.ES.2020.25.3.2000045

The COVID-19 testing debacle. (2020). *Nat Biotechnol, 38*(6), 653-653. doi:10.1038/s41587-020-0575-3

Ferretti, L., Wymant, C., Kendall, M., Zhao, L., Nurtay, A., Abeler-Dörner, L., . . . Fraser, C. (2020). Quantifying SARS-CoV-2 transmission suggests epidemic control with digital contact tracing. *Science, 368*(6491), eabb6936. doi:10.1126/science.abb6936

Gorbalenya, A. E., Baker, S. C., Baric, R. S., de Groot, R. J., Drosten, C., Gulyaeva, A. A., . . . Coronaviridae Study Group of the International Committee on Taxonomy of, V. (2020). The species Severe acute respiratory syndrome-related coronavirus: classifying 2019-nCoV and naming it SARS-CoV-2. *Nature Microbiology*. doi:10.1038/s41564-020-0695-z

Goto, M., Honda, E., Ogura, A., Nomoto, A., & Hanaki, K.-I. (2009). Colorimetric detection of loop-mediated isothermal amplification reaction by using hydroxy naphthol blue. *BioTechniques, 46*(3), 167-172. doi:10.2144/000113072

Hawkins, T. L., O'Connor-Morin, T., Roy, A., & Santillan, C. (1994). DNA purification and isolation using a solid-phase. *Nucleic acids research, 22*(21), 4543-4544. doi:10.1093/nar/22.21.4543

Hsieh, K., Mage, P. L., Csordas, A. T., Eisenstein, M., & Tom Soh, H. (2014). Simultaneous elimination of carryover contamination and detection of DNA with uracil-DNA-glycosylase-supplemented loop-mediated isothermal amplification (UDG-LAMP). *Chemical Communications, 50*(28), 3747-3749. doi:10.1039/C4CC00540F

Jain, N. K., & Roy, I. (2010). Trehalose and protein stability. *Curr Protoc Protein Sci, Chapter 4*, Unit 4.9. doi:10.1002/0471140864.ps0409s59

Jennifer Ong, T. C. E. J., Nathan Tanner. (2015).

Joung, J., Konermann, S., Gootenberg, J. S., Abudayyeh, O. O., Platt, R. J., Brigham, M. D., . . . Zhang, F. (2017). Genome-scale CRISPR-Cas9 knockout and transcriptional activation screening. *Nature Protocols, 12*(4), 828-863. doi:10.1038/nprot.2017.016

Kellner, M. J., Koob, J. G., Gootenberg, J. S., Abudayyeh, O. O., & Zhang, F. (2019). SHERLOCK: nucleic acid detection with CRISPR nucleases. *Nature Protocols, 14*(10), 2986-3012. doi:10.1038/s41596-019-0210-2

Kim, D., Lee, J. Y., Yang, J. S., Kim, J. W., Kim, V. N., & Chang, H. (2020). The Architecture of SARS-CoV-2 Transcriptome. *Cell, 181*(4), 914-921.e910. doi:10.1016/j.cell.2020.04.011

Kwok, S., & Higuchi, R. (1989). Avoiding false positives with PCR. *Nature, 339*(6221), 237-238. doi:10.1038/339237a0

Ladha, A., Joung, J., Abudayyeh, O., Gootenberg, J., & Zhang, F. (2020). A 5-min RNA preparation method for COVID-19 detection with RT-qPCR. *medRxiv*, 2020.2005.2007.20055947. doi:10.1101/2020.05.07.20055947

Lalli, M. A., Chen, X., Langmade, S. J., Fronick, C. C., Sawyer, C. S., Burcea, L. C., . . . Milbrandt, J. (2020). Rapid and extraction-free detection of SARS-CoV-2 from saliva with colorimetric LAMP. *medRxiv*, 2020.2005.2007.20093542. doi:10.1101/2020.05.07.20093542

Niemz, A., Ferguson, T. M., & Boyle, D. S. (2011). Point-of-care nucleic acid testing for infectious diseases. *Trends in Biotechnology, 29*(5), 240-250. doi:https://doi.org/10.1016/j.tibtech.2011.01.007

Notomi, T., Okayama, H., Masubuchi, H., Yonekawa, T., Watanabe, K., Amino, N., & Hase, T. (2000). Loop-mediated isothermal amplification of DNA. *Nucleic acids research, 28*(12), e63-e63. doi:10.1093/nar/28.12.e63

Piepenburg, O., Williams, C. H., Stemple, D. L., & Armes, N. A. (2006). DNA Detection Using Recombination Proteins. *PLOS Biology, 4*(7), e204. doi:10.1371/journal.pbio.0040204

Rabe, B. A., & Cepko, C. (2020). SARS-CoV-2 Detection Using an Isothermal Amplification Reaction and a Rapid, Inexpensive Protocol for Sample Inactivation and Purification. *medRxiv*, 2020.2004.2023.20076877. doi:10.1101/2020.04.23.20076877

Shi, C., Shen, X., Niu, S., & Ma, C. (2015). Innate Reverse Transcriptase Activity of DNA Polymerase for Isothermal RNA Direct Detection. *J Am Chem Soc, 137*(43), 13804-13806. doi:10.1021/jacs.5b08144

Taipale, J., Romer, P., & Linnarsson, S. (2020). Population-scale testing can suppress the spread of COVID-19. *medRxiv*, 2020.2004.2027.20078329. doi:10.1101/2020.04.27.20078329

Tang, Y., Chen, H., & Diao, Y. (2016). Advanced uracil DNA glycosylase-supplemented real-time reverse transcription loop-mediated isothermal amplification (UDG-rRT-LAMP) method for universal and specific detection of Tembusu virus. *Scientific reports, 6*(1), 27605. doi:10.1038/srep27605

Tanner, N. A., Zhang, Y., & Evans, T. C. (2015). Visual detection of isothermal nucleic acid amplification using pH-sensitive dyes. *BioTechniques, 58*(2), 59-68. doi:10.2144/000114253

Wölfel, R., Corman, V. M., Guggemos, W., Seilmaier, M., Zange, S., Müller, M. A., . . . Wendtner, C. (2020). Virological assessment of hospitalized patients with COVID-2019. *Nature, 581*(7809), 465-469. doi:10.1038/s41586-020-2196-x

Zhang, Y., Odiwuor, N., Xiong, J., Sun, L., Nyaruaba, R. O., Wei, H., & Tanner, N. A. (2020). Rapid Molecular Detection of SARS-CoV-2 (COVID-19) Virus RNA Using Colorimetric LAMP. *medRxiv*, 2020.2002.2026.20028373. doi:10.1101/2020.02.26.20028373

Zhang, Y., Ren, G., Buss, J., Barry, A. J., Patton, G. C., & Tanner, N. A. (2020). Enhancing Colorimetric LAMP Amplification Speed and Sensitivity with Guanidine Chloride. *bioRxiv*, 2020.2006.2003.132894. doi:10.1101/2020.06.03.132894

Zou, L., Ruan, F., Huang, M., Liang, L., Huang, H., Hong, Z., . . . Wu, J. (2020). SARS-CoV-2 Viral Load in Upper Respiratory Specimens of Infected Patients. *New England Journal of Medicine, 382*(12), 1177-1179. doi:10.1056/NEJMc2001737

Zou, Y., Mason, M. G., Wang, Y., Wee, E., Turni, C., Blackall, P. J., . . . Botella, J. R. (2017). Nucleic acid purification from plants, animals and microbes in under 30 seconds. *PLOS Biology, 15*(11), e2003916. doi:10.1371/journal.pbio.2003916

Materials and Methods

Clinical sample collection
Nasopharyngeal swabs were collected in 1.5-3 ml VTM, 0.9% NaCl solution or 1x HBSS. Gargle samples were collected from swab-matched patients by letting individuals gargle for 1 minute with 10 ml of HBSS or 0.9% Saline solution. Sputum samples were prepared by mixing sputum material 1:1 with 2x Sputolysin solution (6.5 mM DTT in HBSS) and incubation at room temperature for 15 minutes. Informed consent was obtained from all patients.

RNA extraction from patient material
Total RNA was isolated from 100 µl of nasopharyngeal swabs or cell-enriched gargling solution using a lysis step based on guanidine thiocyanate (adapted from Boom et al. 1990) and 20 µl of carboxylated magnetic beads (GE Healthcare, CAT:65152105050450) applied in 400 µl of Ethanol on the magnetic particle processor

13

KingFisher (Thermo). After a 5-minute incubation at room temperature, DNA was digested with DNaseI for 15 mins at 37°C, followed by a series of wash steps. RNA was eluted from the beads in 50 µl RNase free H$_2$O for 5 minutes at 60°C.

Crude sample inactivation using QuickExtract

50 µl of nasopharyngeal swabs, gargle solution or sputum sample were mixed 1:1 with 2x QuickExtract solution (Lucigen) and heat inactivated for 5 minutes at 95°C. Samples were then stored on ice until further use or frozen at -80°C.

RT-qPCR

For detecting the viral N-gene via RT-qPCR, 1-step RT-qPCR was performed using the SuperScript III Platinum One-Step qRT-PCR Kit (Thermofisher) or Luna Universal One-Step RT-qPCR Kit (NEB) and 1.5 µl of reference primer/probe sets CDC-N1 (IDT 10006713) or CDC-N2 (IDT 10006713) per 20 µl reaction. Reactions were run at 55°C for 15 minutes, 95°C for 2 minutes, followed by 45 cycles of 95°C for 10 seconds and 55°C for 45 seconds in a BioRad CFX qPCR cycler. Each RT-qPCR reaction contained either 5 µl (N-gene, extracted RNA) or 2 µl (N-gene, QuickExtract lysate) of sample input per 20 µl reaction.

Fluorescent RT-LAMP

Fluorescent RT-LAMP reactions were set up using the NEB Warmstart RT-LAMP kit or individual enzymes. For reactions using the RT-LAMP kit, Warmstart RT-LAMP master mix (1x final, 2x stock) was mixed with primer solution (1x final, 10x stock) containing all six LAMP primers (B3, F3, LB, LB, FIP, BIP), LAMP dye (1x final, 50x stock) or Syto9 (1 µM final, 50 µM stock), sample and nuclease-free water. Primers were used at final concentrations of 0.2 µM for F3/B3, 0.4 µM for LB/LF (except for N2 DETECTR, LB/LF 0.8 µM) and 1.6 µM FIP and BIP. Typical final reaction volumes were 10 µl or 20 µl containing 2 µl of sample. For LAMP reactions using individual polymerases, RT-LAMP reactions were set up using NEB 1x Isothermal Amplification Buffer (Bst LF, Bst LF, Bst 3.0) or NEB 1x Isothermal Amplification Buffer II (Bst 3.0), 6 mM MgSO4 (8 mM final; 2 mM MgSO$_4$ are present in Isothermal Buffer I), 0.3 U/µl NEB Warmstart RTx, 0.32 U/µl NEB Bst DNA polymerase (LF, 2.0 or 3.0), 1.4 mM of each dNTP (Larova, 25 mM of each dNTP stock solution), 1x fluorescent dye or 1 µM Syto9, sample and nuclease-free water. Reactions were run at 63°C (62°C for N2 DETECTR and primer comparison) for 30-60 minutes in a BioRad CFX Connect qPCR cycler with SYBR readings every minute.

Preparation of crRNAs for Cas12 detection

LbaCas12a guide RNAs were ordered as reverse complementary Ultramers from IDT. A T7-3G minimal promoter sequence was added for T7 *in vitro* transcription. 1 µM Ultramer was annealed with 1 µM T7-3G oligonucleotide in 1x Taq Buffer (NEB) in a final volume of 10 µl by heating the reaction up to 95°C for 5 minutes, followed by slowly cooling down to 4°C with a 0.8°C/seconds ramp rate. One microliter of 1:10-diluted annealing reaction was used for T7 *in vitro* transcription

using the Invitrogen MEGAScript T7 Transcription kit following the manufacturer instruction. RNA was transcribed for 16 hours at 37°C and purified using AmpureXP RNA beads following instructions described in (Kellner, Koob, Gootenberg, Abudayyeh, & Zhang, 2019).

Cas12-detection of RT-LAMP product

RT-LAMP was set-up as described above and run at 62°C for 60 minutes. Meanwhile, 50 nM purified crRNA was mixed with 62.5 nM EnGen LbCas12 (NEB) in 1x NEB Buffer 2.1 and a final volume of 20 µl. The RNP complex was then incubated for 30 minutes in a heat-block and kept on ice until use. For detection, 2 µl of the RT-LAMP product and 125 nM ssDNA sensor (Invitrogen, DNaseAlert HEX fluorophor) were added to 20 µl of the Cas12-RNP complex on ice. Reporter cleavage was monitored in real-time using a BioRad CFX qPCR cycler with measurements taken every 5 minutes for a total of 60 minutes.

dUTP/UDG contamination prevention system

Reactions were set up to contain NEB 1x Isothermal Amplification Buffer, 1.4 mM of each dATP, dCTP, dGTP, 0.7 mM dUTP, 0.7 mM dTTP, 6 mM MgSO4 (100 mM stock, NEB), 0.32 U/µl NEB Bst 2.0 polymerase, 0.3 U/µl NEB Warmstart RTx Reverse Transcriptase, 0.2 U/µl NEB Antarctic thermolabile UDG, sample and nuclease-free water. Reactions were set up on ice and incubated at room temperature for 5 minutes before being transferred to 63°C to start RT-LAMP reactions under standard conditions described above. For demonstrating carry-over contamination, reactions either contained UDG (+UDG) or water (-UDG) and different amounts of pre-amplified RT-LAMP product (pre-RT-LAMP). Pre-RT-LAMP reactions were performed with dUTP, E-gene primer and 500 copies of Twist synthetic RNA standard for 60 minutes at 63°C. Serial dilutions were made by mixing 1 µl of dUTP-containing pre-RT-LAMP product with 999 µl of nuclease-free water to get 1e3-, 1e6-, 1e9- and 1e12-fold dilutions of pre-RT-LAMP, followed by addition of 2 µl diluted pre-RT-LAMP product to dUTP/UDG RT-LAMP reactions.

Direct sample lysis buffer test

HEK293 cells were trypsinized and counted to make the appropriate dilutions in HBSS. The dilutions were mixed 1:1 with respective lysis buffers and treated as follows: Cells for no extraction were incubated for 5 min at room temperature. QuickExtract samples were incubated at 95°C for 5 min. Cells lysed in the home-made buffer (19.2 mM Tris–HCl (pH 7.8), 1 mM MgCl$_2$, 0.88 mM CaCl$_2$, 20 µM DTT, 2% (wt/vol) Triton X-100) were incubated for 5 min at room temperature before incubation at 95°C for 5 min. For extracted RNA, RNA was purified from 1e5 HEK293 cells using standard Trizol RNA extraction and diluted to cell/reaction equivalents.

Colorimetric LAMP

For HNB colorimetric RT-LAMP detection, reactions were set up as in fluorescent RT-LAMP with the

addition of 120 µM HNB dye solution (20 mM stock in nuclease-free water). Phenol colorimetric reactions were performed using the NEB WarmStart colorimetric LAMP 2x master mix and the same final primer concentrations as in fluorescent RT-LAMP reactions. HNB and Phenol colorimetric reactions further contained 1x fluorescent LAMP dye (50x stock from LAMP kit) or 1 µM Syto9 dye (50 µM Stock) to measure fluorescence in parallel.

Bead-LAMP
For bead enrichment, variable volumes of sample in QuickExtract (60 µl up to 100 µl) were mixed with 0.6x of beads (1:5 dilution of Agencourt RNAClean XP in 2.5 M NaCl, 10 mM Tris-HCl pH 8.0, 20% (w/v) PEG 8000, 0.05% Tween 20, 5 mM NaN$_3$) and incubated for 5 minutes at room temperature. Beads were captured with a magnet for 5 minutes and then washed twice with 85% ethanol for 30 seconds. The beads were air dried for 5 minutes and then eluted directly in 20 µl colorimetric HNB LAMP reaction mix containing 1x NEB WarmStart LAMP kit, 1x Fluorescent LAMP dye, 120 µM HNB dye solution and 1x primer mix. No additional volume for dry beads was factored into the RT-LAMP reaction mix such that reactions were completed with nuclease free water to have final reaction volumes of 20 µl.

As sample input for pooled bead-LAMP (Figure 4F-H, S6A, B), sample pools were prepared by mixing 10 µl of a Covid-19 positive patient gargle sample in QuickExtract with different amounts of a Covid-19 negative gargle sample pool (n=95) in QuickExtract (10 µl per sample). For pool volumes <100 µl, the volume was filled up to 100 µl with HBSS:QuickExtract (1:1); for pool volumes >100 µl, an aliquot of 100 µl was taken out after pooling for subsequent RT-LAMP or bead-LAMP. 40 µl (matching the smallest pooled sample volume) of a Covid-19 positive or negative patient gargle sample were used as positive (qPCR positive) or negative (qPCR negative) controls, and also filled up to 100 µl with HBSS:QuickExtract (1:1) before bead-LAMP.

As sample input for the proof-of-concept experiment shown in Figure S6C-E, sample pools containing different numbers of Covid-19 positive patient gargle sample in QuickExtract were mixed with HeLa cell lysate in QuickExtract. The HeLa cell lysate was prepared by adding 500 µl of HBSS and 500 µl of 2x QuickExtract solution to a HeLa cell pellet containing one million cells, followed by cell lysis for 5 minutes at 95°C. The stock lysate of 1000 cells/µl was then diluted in 1x heat inactivated QuickExtract buffer (diluted to 1x in HBSS) to a final concentration of 20 cells/µl. This concentration was chosen as QuickExtract lysate from gargle or swabs roughly yields 200 pg/µl of RNA or 20 cells/µl. This Covid-19 negative QuickExtract lysate was used to spike-in various amounts of Covid-19 positive patient QuickExtract lysate.

Assessment of bead enrichment
For evaluation of the recovery rate after bead enrichment different dilutions of Twist synthetic SARS-CoV-2 RNA standard were made in HeLa cell lysate. 40 µl of sample was adjusted to 100 µl with QuickExtract diluted 1:1 with HBSS. Bead enrichment was performed as described for bead-LAMP. Nucleic acids were eluted with 20 µl nuclease-free water for 5 minutes at 63˚C. SARS-CoV-2 RNA concentrations were determined in the input (before enrichment) and eluate (after bead enrichment) by RT-qPCR.

HomeDip-LAMP
Reactions for HomeDip-LAMP were set up as for HNB colorimetric LAMP, with final reaction volumes (excluding sample volume) being 25 µl. Filter paper dipsticks (dimensions: 2x10 mm) were cut from filter paper (Fisher Scientific, cat. number 09-790-14D). Using forceps, dipsticks were dipped into 2 µl of patient sample for 30 seconds, allowing the liquid to be drawn entirely onto the paper. The paper strips were then washed by rapidly submerging ('dipping') three times into wash solution, typically 130 mM NaCl. Sample strips were then dipped three times into the PCR tubes containing 25 µl of pre-distributed HNB RT-LAMP reaction mixes. The RT-LAMP reaction was performed for 30 minutes in a water bath that was temperature-controlled by a sous-vide heater (Allpax) set to 63°C. PCR tubes were kept upright and submerged during incubation by floating pipette tip racks.

Assessment of SARS-CoV-2 detection rates (related to Discussion)
Measured RT-qPCR Cq values from clinical samples presented in Figure 2B and 2F were transformed to copies per reaction using Cq 30 = 1000 copies/reaction (determined in Figure S5A) as reference. For calculations, entire swab volumes were set to 3 ml, from which 100 µl were used for RNA extractions (eluted in 50 µl; 5 µl of RNA per RT-qPCR) and bead-LAMP. QuickExtract lysates were prepared with 2x buffer, and 2 µl were used for RT-qPCR or RT-LAMP. Copies per reaction were then transformed to equivalent copies per original sample volume used for reactions (20 µl for extracted RNA, 1 µl of QuickExtract crude lysate), and projected to 3 ml total swab volumes. Detection rates were calculated by dividing the number of detected samples for each procedure by the total number of detected individuals measured by RT-qPCR on extracted RNA (most sensitive method). A robust detection limit of 100 copies/reaction was used for RT-LAMP, and 5 copies/reaction for RT-qPCR. Depending on the respective purification strategy, up to 100x fold enrichment can be achieved (bead-LAMP) from 100 µl original sample.

15

Primer sequences

Primer sequences for RT-LAMP

name	sequence	reference
DETECTR N-gene F3	AACACAAGCTTTCGGCAG	(Broughton et al., 2020)
DETECTR N-gene B3	GAAATTTGGATCTTTGTCATCC	
DETECTR N-gene FIP	TGCGGCCAATGTTTGTAATCAGCCAAGGAAATTTTGGGGAC	
DETECTR N-gene BIP	CGCATTGGCATGGAAGTCACTTTGATGGCACCTGTGTAG	
DETECTR N-gene LF	TTCCTTGTCTGATTAGTTC	
DETECTR N-gene LB	ACCTTCGGGAACGTGGTT	
NEB E1-F3	TGAGTACGAACTTATGTACTCAT	(Zhang, Ren, et al., 2020)
NEB E1-B3	TTCAGATTTTTAACACGAGAGT	
NEB E1-FIP	ACCACGAAAGCAAGAAAAAGAAGTTCGTTTCGGAAGAGACAG	
NEB E1-BIP	TTGCTAGTTACACTAGCCATCCTTAGGTTTTACAAGACTCACGT	
NEB E1-LB	GCGCTTCGATTGTGTGCGT	
NEB E1-LF	CGCTATTAACTATTAACG	
As1_F3	CGGTGGACAAATTGTCAC	(Rabe & Cepko, 2020)
As1_B3	CTTCTCTGGATTTAACACACTT	
As1_LF	TTACAAGCTTAAAGAATGTCTGAACACT	
As1_LB	TTGAATTTAGGTGAAACATTTGTCACG	
As1_FIP	TCAGCACACAAAGCCAAAAATTTATCTGTGCAAAGGAAATTAAGGAG	
As1_BIP	TATTGGTGGAGCTAAACTTAAAGCCCTGTACAATCCCTTTGAGTG	
As1e_FIP	TCAGCACACAAAGCCAAAAATTTATTTTTCTGTGCAAAGGAAATTAAGGAG	
As1e_BIP	TATTGGTGGAGCTAAACTTAAAGCCTTTTCTGTACAATCCCTTTGAGTG	
NEB N-gene-A-F3	TGGCTACTACCGAAGAGCT	(Zhang, Odiwuor, et al., 2020)
NEB N-gene-A-B3	TGCAGCATTGTTAGCAGGAT	
NEB N-gene-A-FIP	TCTGGCCCAGTTCCTAGGTAGTCCAGACGAATTCGTGGTGG	
NEB N-gene-A-BIP	AGACGGCATCATATGGGTTGCACGGGTGCCAATGTGATCT	
NEB N-gene-A-LF	GGACTGAGATCTTTCATTTTACCGT	
NEB N-gene-A-LB	ACTGAGGGAGCCTTGAATACA	
NEB N2-F3	ACCAGGAACTAATCAGACAAG	(Zhang, Ren, et al., 2020)
NEB N2-B3	GACTTGATCTTTGAAATTTGGATCT	
NEB N2-FIP	TTCCGAAGAACGCTGAAGCGGAACTGATTACAAACATTGGCC	
NEB N2-BIP	CGCATTGGCATGGAAGTCACAATTTGATGGCACCTGTGTA	
NEB N2-LF	GGGGGCAAATTGTGCAATTTG	
NEB N2-LB	CTTCGGGAACGTGGTTGACC	
Mammoth RNaseP POP7 F3	TTGATGAGCTGGAGCCA	(Broughton et al., 2020)
Mammoth RNaseP POP7 B3	CACCCTCAATGCAGAGTC	
Mammoth RNaseP POP7 FIP	GTGTGACCCTGAAGACTCGGTTTTAGCCACTGACTCGGATC	
Mammoth RNaseP POP7 BIP	CCTCCGTGATATGGCTCTTCGTTTTTTTCTTACATGGCTCTGGTC	
Mammoth RNaseP POP7 LF	ATGTGGATGGCTGAGTTGTT	
Mammoth RNaseP POP7 LB	CATGCTGAGTACTGGACCTC	
ACTB-F3	AGTACCCCATCGAGCACG	(Zhang, Ren, et al., 2020)
ACTB-B3	AGCCTGGATAGCAACGTACA	
ACTB-FIP	GAGCCACACGCAGCTCATTGTATCACCAACTGGGACGACA	
ACTB-BIP	CTGAACCCCAAGGCCAACCGGCTGGGGTGTTGAAGGTC	
ACTB-LoopF	TGTGGTGCCAGATTTTCTCCA	
ACTB-LoopB	CGAGAAGATGACCCAGATCATGT	

RT-qPCR primers and probes

name	sequence	reference
CDC-N1-F	GACCCCAAAATCAGCGAAAT	CDC
CDC-N1-R	TCTGGTTACTGCCAGTTGAATCTG	CDC
CDC-N1-P	FAM-ACCCCGCATTACGTTTGGTGGACC-BHQ1	CDC
CDC-N2-F	TTACAAACATTGGCCGCA AA	CDC
CDC-N2-R	GCGCGACATTCCGAAGAA	CDC
CDC-N2-P	FAM-ACAATTTGCCCCCAGCGCTTCAG-BHQ1	CDC

Oligos for crRNAs for LbaCas12a

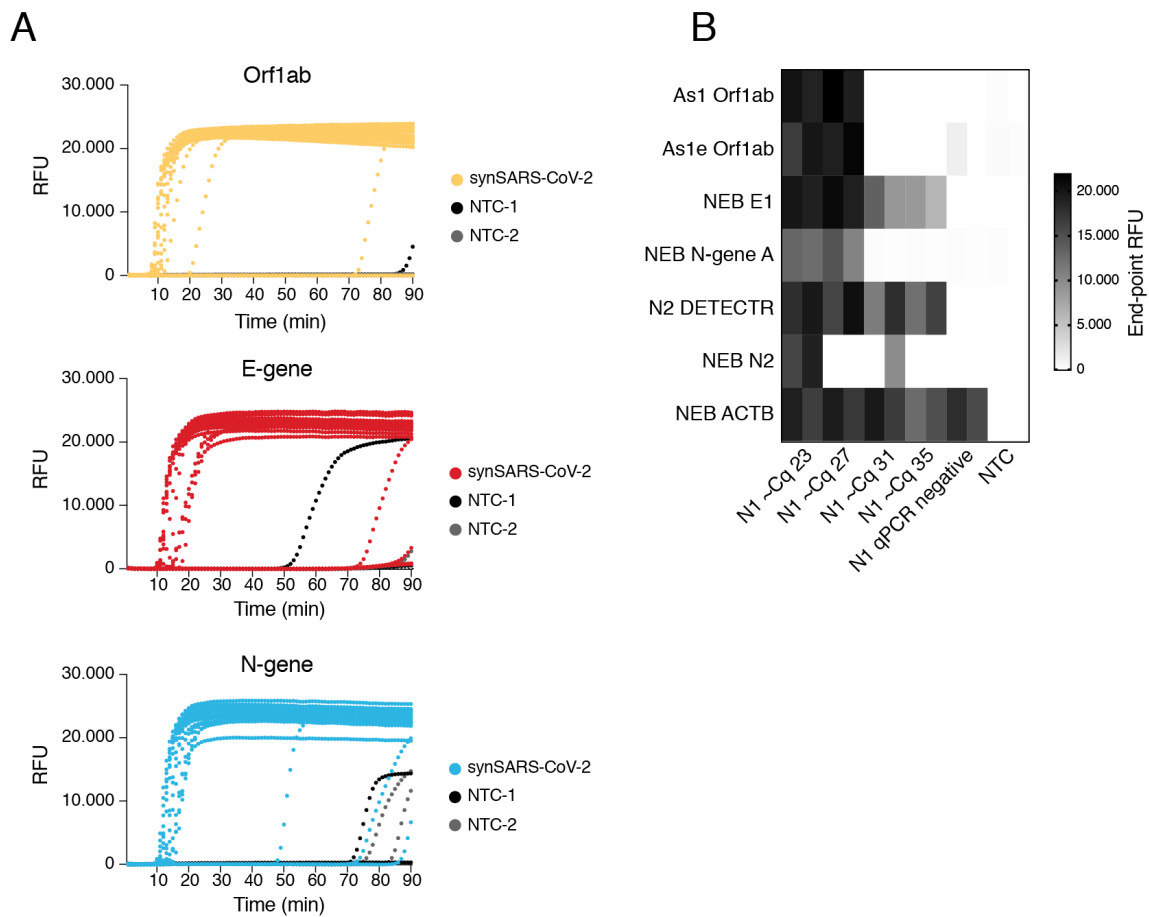| name	sequence	reference
DETECTR N-gene LbaCas12a guide	GAACGCTGAAGCGCTGGGGGATCTACACTTAGTAGAAATTAcccctatagtgagtcgtattaatttc	(Broughton et al., 2020)
T7-3G IVT primer	GAAATTAATACGACTCACTATAGGG	(Kellner et al., 2019)

Supplementary Figures

Figure S1

Figure S1. Primer performance for the detection of SARS-CoV-2 by RT-LAMP. A) Amplification curves (real-time fluorescent measurements; in duplicates) from RT-LAMP reactions shown in Figure 1C. Curves using synthetic SARS-CoV-2 RNA standard dilutions as input are in color (color-code indicates different primer sets; yellow: As1 Orf1ab; red: E-gene E1 NEB; blue: N-gene N2 DETECTR). Curves using non-targeting controls (NTC) as input are shown in black. **B)** Heatmap showing end-point relative fluorescence values (after 35 minutes) of RT-LAMP reactions (in duplicates; respective primers indicated to the left) using Covid-19 patient samples with indicated Cq values (determined via RT-qPCR and the N1-CDC amplicon) as input. Reactions with primers targeting the human ACTB gene served as sample quality control. All reactions were performed in duplicates.
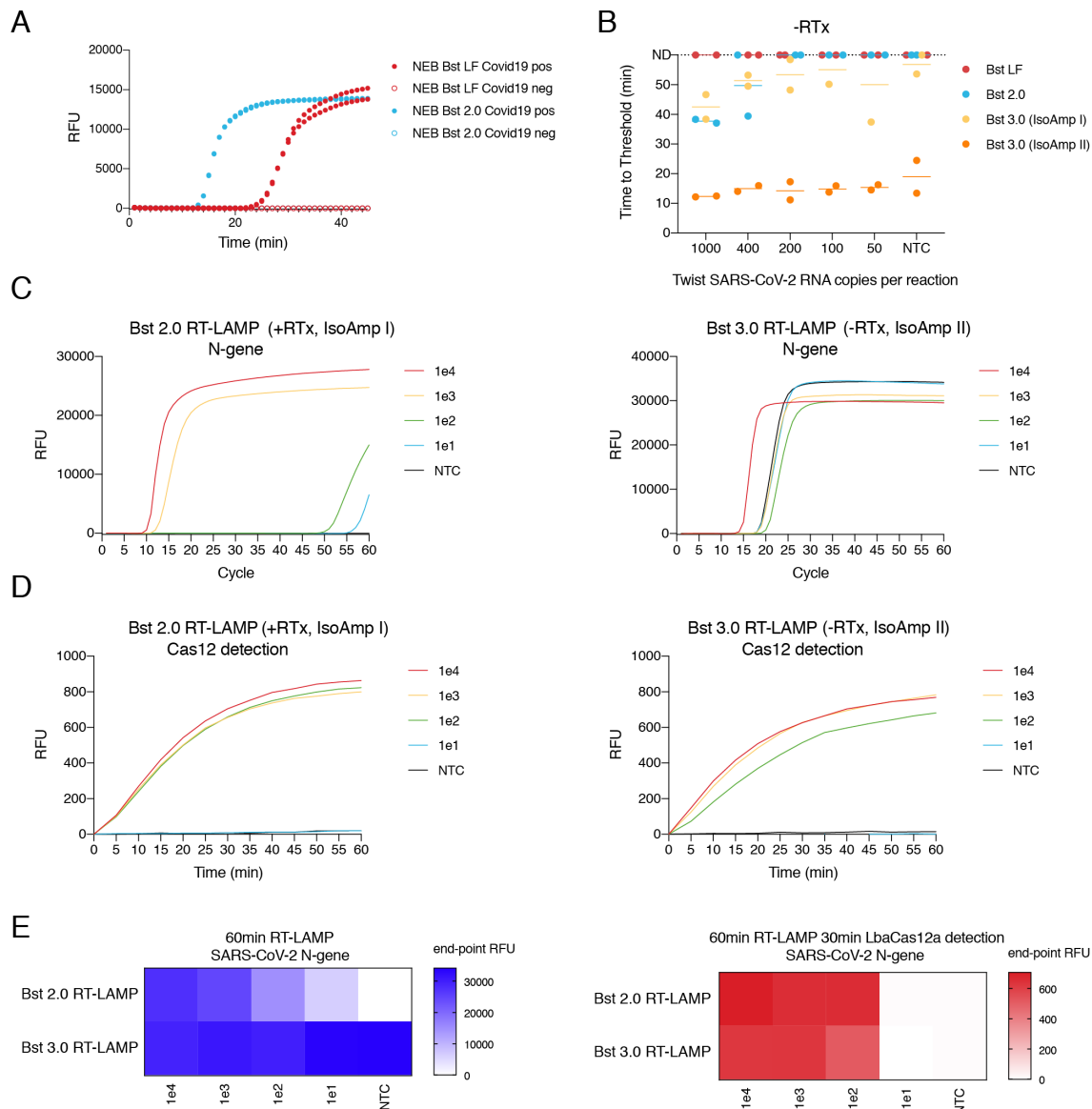
Figure S2

Figure S2. Benchmarking Bst polymerases for RT-LAMP. A) Performance of Bst LF (red curves) or Bst 2.0 (blue curves) on crude Covid-19 patient sample (prepared in QuickExtract). Amplification curves indicate real-time fluorescence measurements of RT-LAMP reactions (E1 primer set; in duplicates) using SARS-CoV-2 positive (filled circles) or SARS-CoV-2 negative (open circles) patient samples as input. **B)** LAMP performance (given as time to threshold in minutes) of indicated Bst DNA polymerase variants in the absence of a dedicated reverse transcriptase using diluted synthetic SARS-CoV-2 RNA (copies per reaction indicated) as template (related to Figure 1D). **C)** RT-LAMP real-time fluorescence measurements using RTx and Bst 2.0 in IsoAmp buffer I (left) versus Bst 3.0 alone in IsoAmp buffer II (right). N2 DETECTR was used as primer set for amplifying synthetic SARS-CoV-2 RNA standard (copy number per reaction indicated; no target control (NTC): water). **D)** Shown is the collateral cleavage activity (measured as real-time fluorescent signal) by Cas12, with a crRNA targeting the N2 LAMP amplicon, upon addition of 2 µl of LAMP reactions from C) to 20 µl of Cas12 cleavage mix. **E)** (Left) End-point fluorescence values (after 60 minutes) of RT-LAMP reactions from C). (Right) Cas12-based detection of LAMP products from D) is indicated.
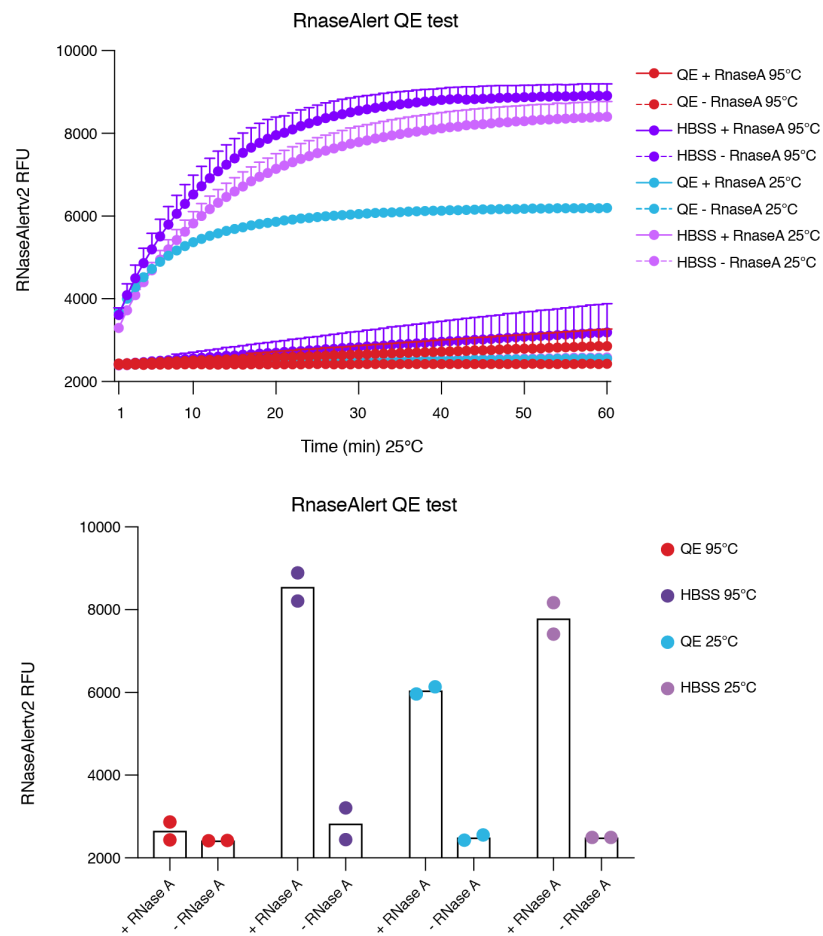
18

Figure S3

Figure S3. QuickExtract buffer combined with heat inhibits RNase activity. Shown are relative fluorescence values over time (upper graph) and end-point fluorescence values (lower graph) of RNaseAlert reactions in HBSS buffer or 1x QuickExtract, in the presence or absence of RNaseA and with or without incubation at 95°C. All reactions were performed in duplicates.
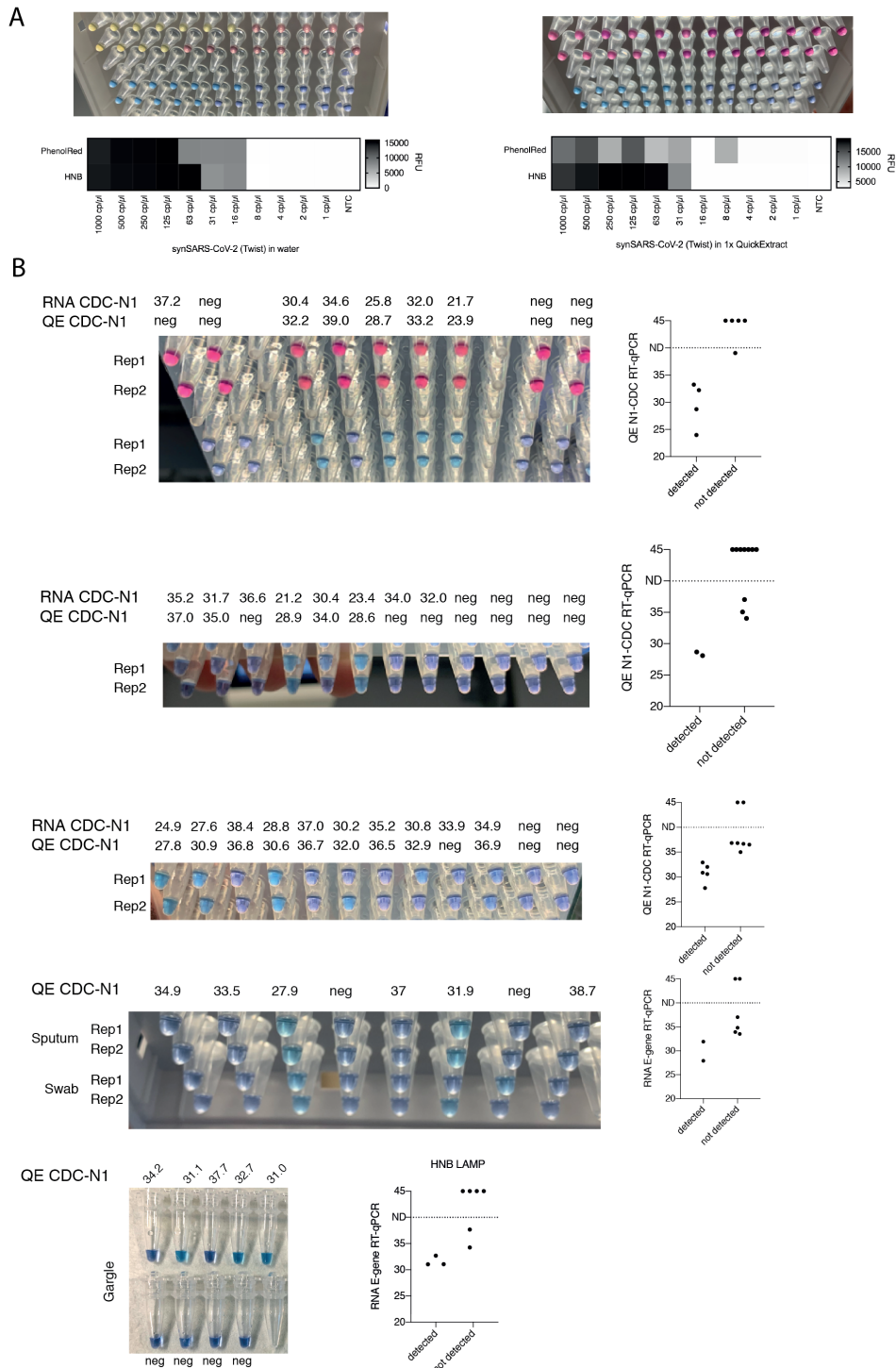
Figure S4

Figure S4: HNB RT-LAMP shows robust performance on QuickExtract-treated patient sample material.
A) Comparison between Phenol Red and HNB colorimetric readout of RT-LAMP reactions (in duplicates) on serially diluted synthetic SARS-CoV-2 RNA in water (left) or 1x QuickExtract (right). End-point fluorescence values measured in parallel are shown in heatmaps below. While fluorescent detection indicates successful LAMP in both sample matrices, Phenol Red but not HNB colorimetric readout is inconclusive in QuickExtract buffer (right panel, top rows). **B)** HNB RT-LAMP performance across a wide range of Covid-19 patients and sample types. Images showing the HNB end-point outcome of RT-LAMP reactions on multiple Covid-19 patient samples (gargle, swab or sputum; samples indicate swabs if not otherwise stated). The respective Cq values of the individual samples (CDC-N1; QuickExtract RT-qPCR) are shown above each sample. Colorimetric RT-LAMP using Phenol Red is shown for one sample set (first from top), again with inconclusive outcome. All reactions were performed in duplicates. Summary dotplots for every sample set are shown to the right; samples were classified as detected or not detected based on RT-LAMP outcome and plotted against their respective RT-qPCR determined Cq values.
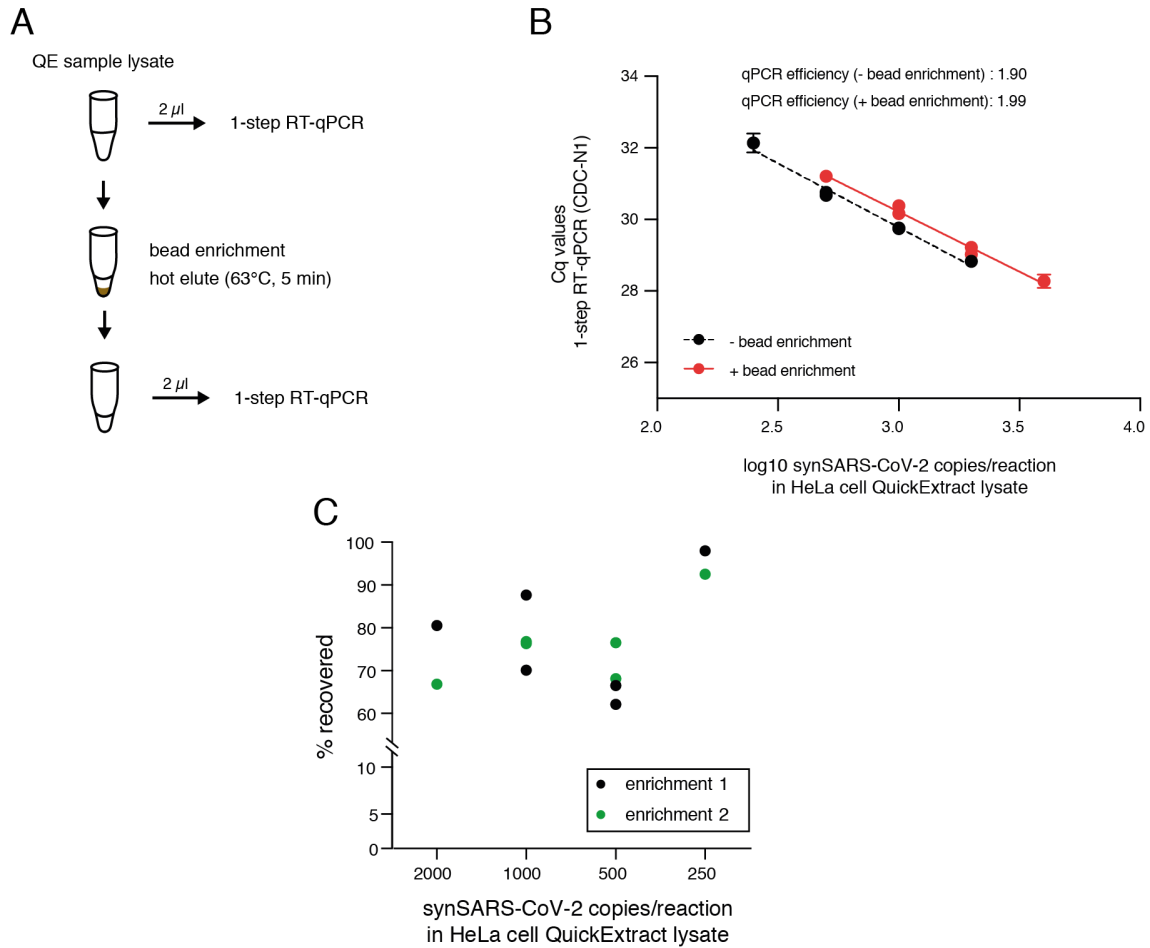
Figure S5

Figure S5: Assessment of the bead enrichment procedure.
A) Schematic depicting the workflow to asses bead recovery performance. Synthetic SARS-CoV-2 standard was diluted in HBSS:QuickExtract lysis buffer (1:1). 40 µl were subjected to magnetic bead enrichment, followed by elution of nucleic acids in 20 µl of RNase-free water by incubation at 63˚C for 5 min. 2 µl of the input (before enrichment) and the eluate (after bead enrichment) were analysed by 1-step RT-qPCR. **B)** RT-qPCR Cq values of different dilutions of synthetic SARS-CoV-2 standard before (black) and after bead enrichment (red). Duplicate experiments are shown. qPCR efficiency was calculated as $10^{(-1/slope)}$ of the linear regression of datapoints). **C)** Calculated recovery (in %) after bead enrichment for the dilution series of synthetic SARS-CoV-2 RNA standard measured in B) per enrichment reaction. Replicate experiments are shown in black and green.
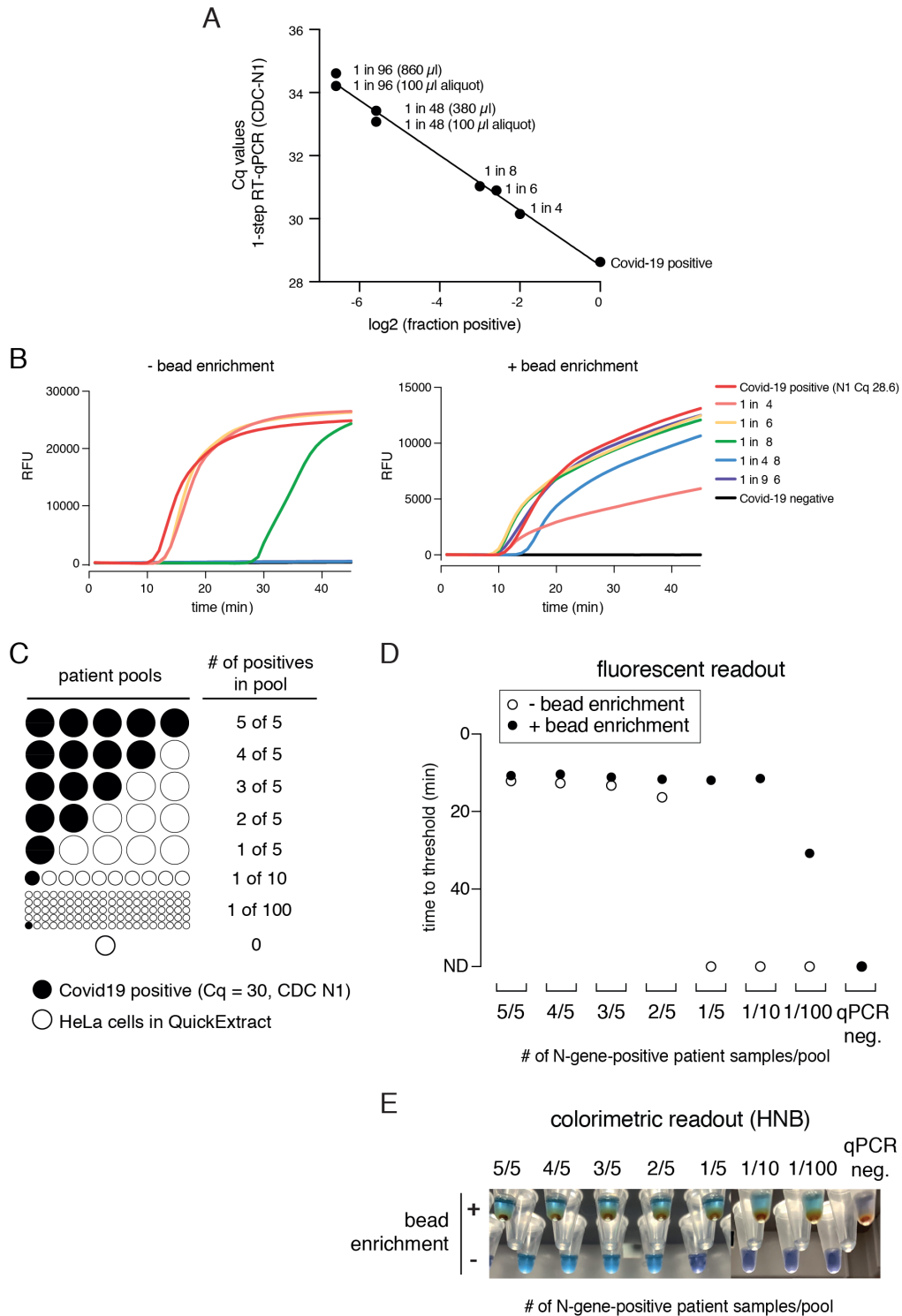
Figure S6

Figure S6: Pooled Covid-19 testing strategy using bead-LAMP.
A) RT-qPCR Cq values (CDC-N1) of gargle sample pools used in Fig 4F-H with the indicated fraction of Covid-19 positive gargle sample per pool. For the two large sample pools (pool of 1 in 96 and pool of 1 in 48), the 100 μl aliquot used for subsequent RT-LAMP and bead-LAMP was measured in addition. **B)** Readout of a real-time fluorescence RT-LAMP reaction of sample pools with indicated fraction of positive lysate without (left) and with (right) bead enrichment. RFU: relative fluorescent units. **C)** Schematic illustrating the pooled testing strategy. Eight pools mimicking different total patient sample numbers and different ratios of Covid-19-positive patient samples (0-100%) were generated from one Covid-19-positive QuickExtract patient sample (N1 RT-qPCR with Cq ~30) mixed at the indicated ratios with QuickExtract HeLa cell lysate at 20 cells/μl. **D)** Shown is the performance (measured as end-point relative fluorescence units (RFU)) of bead-LAMP (filled circles) compared to regular RT-LAMP (open circles) on the patient pools defined in A). ND = not detected within 60 minutes of RT-LAMP incubation. **E)** Images showing the endpoint HNB colorimetric readout of samples measured in B) with or without prior bead enrichment.
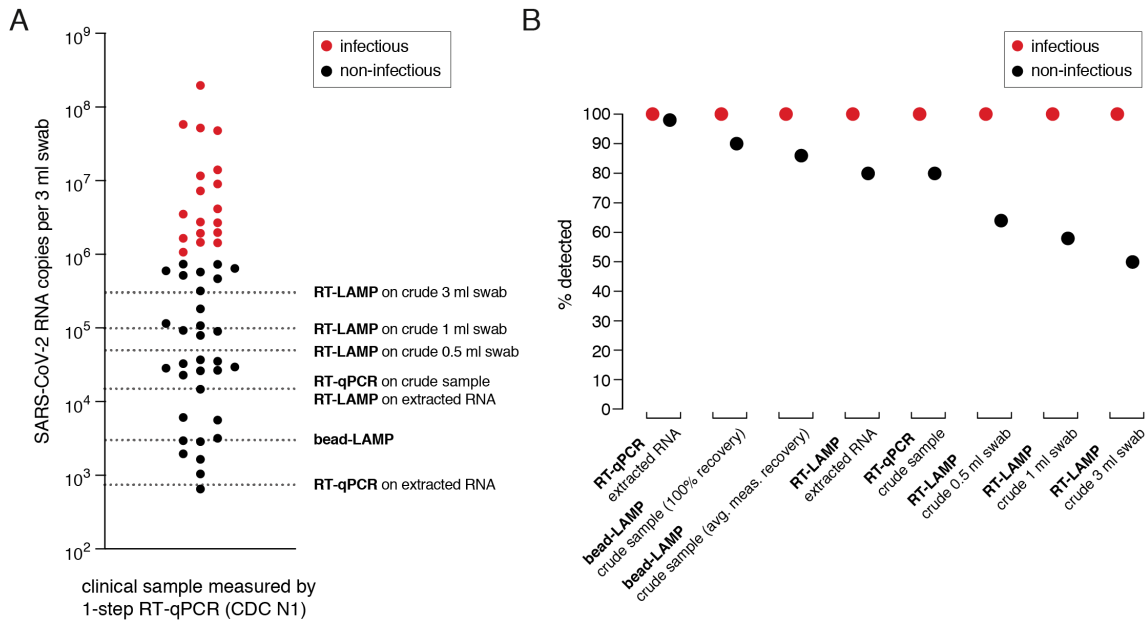
Figure S7

Figure S7: Potential of RT-LAMP-based assays for clinical SARS-CoV-2 diagnostics.
A) Hypothetical performance of RT-LAMP-based assays based on copy numbers of SARS-CoV-2 RNA (measured by RT-qPCR) in patient samples derived from nasopharyngeal swabs in 3 ml transport medium. Copy numbers per 3 ml swab were calculated from estimated copies per reaction measured by 1-step RT-qPCR using Cq 30 = 1000 copies/ reaction as reference (Figure S5 process control). Dashed lines indicate threshold detection levels for each procedure when considering 20 µl of original sample for RT-qPCR and RT-LAMP on extracted RNA (from 100 µl original sample eluted in 50 µl), 100 µl of original sample for bead-LAMP, and 1 µl of original sample for RT-LAMP and RT-qPCR on crude lysate. Patients were classified as infectious (red) if copies per swab were >1e6 (Wölfel et al., 2020). **B)** Hypothetical detection rates of RT-qPCR and various RT-LAMP-based assays with regards to infectivity based on the data shown in A). For bead-LAMP, detection rates considering maximal nucleic acid recovery rates (100%) and measured average nucleic acid recovery rates (77%) are shown.